Table 1: List of "apoptosis" genes selectively upregulated in cluster 3

Gene Symbol	Gene Name	Entrez Gene No.	2 hr	6 hr	12 hr	24 hr	48 hr	72 hr
Nr4a2	nuclear receptor subfamily 4, group A, member 2	54278	1.60	**4.29**	1.30	**2.97**	**6.14**	**7.39**
Fosl1	fos-like antigen 1	25445	1.69	**2.09**	**2.15**	**2.34**	**3.02**	**6.46**
Itgav	integrin alpha V	296456	1.39	1.56	**2.78**	**2.38**	**5.32**	**5.22**
Twist2	twist homolog 2 (Drosophila)	59327	1.42	1.50	1.37	1.58	**3.08**	**4.84**
Rarb	retinoic acid receptor, beta	24706	0.89	0.83	1.42	1.80	**3.90**	**4.24**
Dusp1	dual specificity phosphatase 1	114856	0.96	1.70	1.89	1.47	**2.59**	**4.16**
Hmox1	heme oxygenase (decycling) 1	24451	1.63	**2.86**	**3.07**	**2.62**	**2.25**	**3.71**
Angptl4	angiopoietin-like 4	362850	1.23	1.28	1.33	1.98	**2.73**	**3.60**
Acin1	apoptotic chromatin condensation inducer 1	305884	0.92	0.67	1.31	**2.14**	**2.68**	**3.41**
Pdgfrb	Platelet derived growth factor receptor, beta polypeptide	24629	0.84	0.77	1.71	1.92	**2.99**	**3.26**
Gclc	glutamate-cysteine ligase, catalytic subunit	25283	1.25	1.99	1.58	1.80	**2.02**	**3.01**
Ihpk2	inositol hexaphosphate kinase 2	59268	1.07	1.17	1.26	1.64	**2.39**	**2.88**
Dapk1	death associated protein kinase 1	306722	0.85	0.95	1.55	1.38	**2.70**	**2.82**
Amigo2	adhesion molecule with Ig like domain 2	300186	0.87	0.93	1.00	1.33	1.49	**2.81**
Mmp2	matrix metallopeptidase 2	81686	1.05	1.12	1.32	1.48	1.92	**2.76**
Hipk2	Homeodomain interacting protein kinase 2	362342	1.01	1.63	2.14	1.86	**2.94**	**2.69**
Birc3	baculoviral IAP repeat-containing 3	78971	1.52	1.63	1.22	1.48	**2.27**	**2.68**
Myd116	myeloid differentiation primary response gene 116	171071	1.09	1.90	2.17	1.58	**2.95**	**2.67**
Il1rn	interleukin 1 receptor antagonist	60582	1.73	**2.51**	**3.06**	1.77	**3.57**	**2.49**
Hipk1	homeodomain interacting protein kinase 1	365895	1.12	1.05	1.30	1.37	**2.44**	**2.48**
LOC687118	similar to death effector domain-containing DNA binding protein 2	687118	1.58	1.58	**2.14**	**2.00**	**3.13**	**2.46**
Ripk2	receptor (TNFRSF)-interacting serine-threonine kinase 2	362491	1.04	1.33	1.48	1.69	**2.55**	**2.38**
Dapk1	death associated protein kinase 1	306722	0.97	1.00	1.16	1.35	**2.16**	**2.35**
Timp3	Tissue inhibitor of metalloproteinase 3	25358	1.16	1.08	1.28	1.01	1.78	**2.35**
Cln3	ceroid lipofuscinosis, neuronal 3, juvenile (Batten, Spielmeyer-Vogt disease)	293485	1.17	1.56	**2.08**	1.50	**2.44**	**2.32**
Ercc5	excision repair cross-complementing rodent repair deficiency, complementation group 5	301382	1.05	1.29	1.30	**2.06**	**2.13**	**2.28**
Pik3ca	phosphatidylinositol 3-kinase, catalytic, alpha polypeptide	170911	1.08	1.05	1.45	1.63	**2.07**	**2.20**
Raf1	v-raf-leukemia viral oncogene 1	24703	1.13	1.66	1.71	1.73	**2.01**	**2.17**
Ednrb	endothelin receptor type B	50672	1.32	1.09	1.46	1.94	1.31	**2.15**
Cd24	CD24 molecule	25145	0.78	0.61	0.70	0.71	1.39	**2.13**
Hipk2	homeodomain interacting protein kinase 2	362342	0.93	0.99	1.47	1.35	**2.33**	**2.09**
Timp3	Tissue inhibitor of metalloproteinase 3	25358	1.10	0.85	1.13	0.98	1.36	**2.08**
Vegfa	vascular endothelial growth factor A	83785	0.89	1.20	0.94	1.09	**2.02**	**2.07**
Gal	galanin	29141	1.32	1.22	1.85	0.77	1.84	**2.03**
Furin	furin (paired basic amino acid cleaving enzyme)	54281	1.17	1.20	1.36	1.18	1.89	**2.03**
Ep300	E1A binding protein p300	170915	1.33	1.09	1.23	1.29	**2.28**	**2.01**
Sh3kbp1	SH3-domain kinase binding protein 1	84357	1.03	1.58	1.78	1.47	**2.52**	1.85
Psen2	presenilin 2	81751	1.37	1.52	**2.14**	1.91	**2.09**	1.81
Ptk2b	PTK2 protein tyrosine kinase 2 beta	50646	0.93	1.29	1.95	1.69	**2.17**	1.81
LOC687813	similar to Tnf receptor-associated factor 1	687813	1.87	**2.36**	**2.35**	1.68	**2.71**	1.75
Ncf1	neutrophil cytosolic factor 1	114553	1.83	**2.78**	**2.72**	**2.44**	**2.59**	1.75

Table 1: List of "apoptosis" genes selectively upregulated in cluster 3 (Continued)

Apbb2	amyloid beta (A4) precursor protein-binding, family B, member 2	305338	1.09	1.12	1.48	1.28	**2.15**	1.74
Cln8	ceroid-lipofuscinosis, neuronal 8	306619	1.52	**2.11**	**2.21**	1.77	1.94	1.73
Sh3kbp1	SH3-domain kinase binding protein 1	84357	1.15	1.41	1.47	1.58	**2.41**	1.72

[28]. A load stimulus is detected by a mechano-electrochemical sensory system, including mechanically sensitive ion channels (stretch-activated channels) linked to the cytoskeleton [29]. The principle detection system is the matrix-integrin-mechanosensory protein complex-cytoskeleton machinery [30,31]. This system is linked to the kinase cascade (tyrosine or nontyrosine kinase cascade or the JAK/STAT kinase cascade) system, which provides amplification, diversity, selectivity, and modulation capabilities and contains focal adhesion kinase (FAK) [32]. The Src homology protein complex (SHC) and growth factor receptor binding adaptor protein linking receptor (GRB2) link to the Ras-raf signaling pathway, and these are regulated through FAK. Ras and GTPase activation regulates the activation of Raf, MAPK and extracellular regulated kinase (ERK) [33,34]. Activated ERKs enter the nucleus and upregulate the expression of various transcription factors (jun, fos, myc, erg-1) and activate nuclear binding proteins such as NF-κB [35]. Specific regulation may occur at load response elements in promoters of certain genes such as platelet-derived growth factor (PDGF) [36]. The mechanically sensitive ion channel could also be a gap junction channel, which propagates a Ca^{2+} wave from cell to cell after a mechanical signal is detected through a cell adhesion molecule (CAM).

It is clear that systems involved in evoking the response of neuronal cells to applied mechanical load are highly complex, which requires an expansive approach to their elucidation. Our results in primary neuronal-rich culture have analyzed gene expression profiles using the Affymatrix system and thereby have identified 3,412 genes with altered expression as a result of applied cyclic tensile stress, many of which are consistent with previous studies. These data will be useful for future examination of how the effects of mechanical insult on the spinal cord, in particular, are regulated. Signalling pathways that may be involved in this process can be modulated by molecules such as G proteins, kinase phosphorylation and activation, and kinase inhibitors or phosphatases [34]. Indeed, the MAPK kinase pathway was identified by KEGG analysis of the alterations in gene expression seen in the

Table 2: List of "response to stimulus" genes selectively upregulated in cluster 1

Gene Symbol	Gene Name	Entrez Gene No.	2 hr	6 hr	12 hr	24 hr	48 hr	72 hr
Serpina3n	serine (or cysteine) peptidase inhibitor, clade A, member 3N	24795	1.53	**2.52**	**3.13**	**5.38**	**20.18**	**49.34**
Ereg	epiregulin	59325	1.99	**3.65**	**2.75**	**3.06**	**9.51**	**37.80**
Ptgs2	prostaglandin-endoperoxide synthase 2	29527	1.55	**3.81**	**2.35**	**3.48**	**12.52**	**21.58**
Ccl20	chemokine (C-C motif) ligand 20	29538	1.20	**2.27**	**2.07**	1.83	**8.52**	**20.38**
Cxcl3	chemokine (C-X-C motif) ligand 3	171551	1.62	**2.54**	**3.06**	**2.67**	**7.10**	**18.43**
Hspa4l	heat shock protein 4 like	294993	0.80	0.62	**2.19**	1.19	**4.98**	**7.69**
Grem1	gremlin 1	50566	1.11	1.45	1.12	**2.19**	**2.23**	**7.69**
Nupr1	nuclear protein 1	113900	0.93	0.81	1.69	1.34	**4.49**	**6.11**
Cryab	crystallin, alpha B	25420	0.83	0.88	1.35	1.06	**3.03**	**5.96**
Gls	glutaminase	24398	1.00	1.15	1.89	1.73	**3.80**	**5.44**
Cyp4b1	cytochrome P450, family 4, subfamily b, polypeptide 1	24307	0.72	1.75	1.26	0.66	1.42	**5.18**
Sncg	synuclein, gamma	64347	0.95	0.77	0.92	1.12	**2.72**	**4.71**
Vnn1	vanin 1	29142	1.10	1.37	1.43	1.31	1.64	**4.71**
Gls	glutaminase	24398	0.88	0.94	0.79	0.92	1.66	**3.89**
Cxcl10	chemokine (C-X-C motif) ligand 10	245920	1.23	1.01	0.84	1.08	1.65	**3.41**
Inhbb	Inhibin beta-B	25196	0.97	1.01	1.14	1.32	0.97	**3.28**
Slc12a2	solute carrier family 12 (sodium/potassium/chloride transporters), member 2	83629	0.88	0.88	0.97	0.88	1.58	**3.07**

Table 3: High frequency pathways* identified by KEGG/ pathway analysis in clusters 1, 2, and 3

rank	pathway (total gene count)	p-value	count
cluster 1			
1	Glutamate metabolism (26)	0.0021	2
2	D-Glutamine and D-glutamate metabolism (3)	0.0081	1
3	Taurine and hypotaurine metabolism (10)	0.0266	1
4	Pantothenate and CoA biosynthesis (11)	0.0293	1
cluster 2			
1	T cell receptor signaling pathway (95)	0.0156	2
2	Glycosphingolipid biosynthesis - ganglio series (15)	0.0307	1
3	Cell adhesion molecules (CAMs) (151)	0.0371	2
cluster 3			
1	Focal adhesion (187)	0.0001	17
2	Bladder cancer (36)	0.0001	7
3	TGF-beta signaling pathway (81)	0.0003	10
4	Pathways in cancer (313)	0.0005	22
5	Prostate cancer (92)	0.0008	10
6	Small cell lung cancer (92)	0.0008	10
7	ECM-receptor interaction (74)	0.0028	8
8	Glioma (64)	0.0047	7
9	Melanoma (69)	0.0072	7
10	Renal cell carcinoma (69)	0.0072	7
11	PPAR signaling pathway (70)	0.0078	7
12	mTOR signaling pathway (54)	0.0081	6
13	Gap junction (90)	0.0091	8
14	Glycerophospholipid metabolism (46)	0.0168	5
15	MAPK signaling pathway (255)	0.0200	15
16	Non-small cell lung cancer (52)	0.0273	5
17	Pancreatic cancer (71)	0.0286	6
18	GnRH signaling pathway (91)	0.0296	7
19	Adherens junction (73)	0.0323	6
20	Pyruvate metabolism (38)	0.0351	4
21	Regulation of actin cytoskeleton (204)	0.0357	12
22	Leukocyte transendothelial migration (116)	0.0366	8
23	Chronic myeloid leukemia (79)	0.0449	6
24	Glutathione metabolism (42)	0.0482	4

*, Listed pathways are all statistically significant ($P < 0.05$). "total gene count" means the number of genes in each pathway, which have already been registered in KEGG system, and "count" means the number of genes, which were expressed significantly in each pathway in this study.

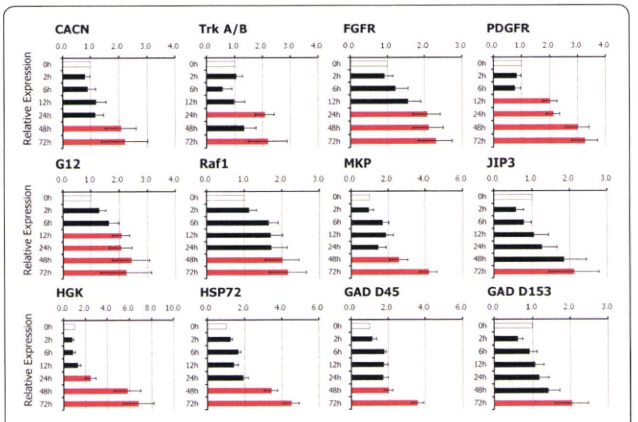

Figure 4 The effects of cyclic tensile stress on gene expression levels analyzed by real time RT-PCR. Application of cyclic tensile stress resulted in significant increases in mRNA expression levels of platelet derived growth factor receptor (PDGFR), guanine nucleotide binding protein gamma 12 (G12) at 12 hours, neurotrophic tyrosine kinase receptor type 2 (trkA/B), fibroblast growth factor receptor (FGFR), mitogen-activated protein kinase kinase kinase kinase 4 (HGK) at 24 hours, and calcium channel voltage-dependent L type alpha 1F subunit (CACN), v-raf-leukemia viral oncogene 1 (Raf1), dual specificity phosphatase 1 (MKP), mitogen-activated protein kinase 8 interacting protein 3 (JIP3), heat shock protein 72 (HSP72), DNA-damage-inducible alpha (GAD D45), DNA-damage inducible transcript 3 (GAD D153) at 48-72 hours. Red bars indicate significant differences ($P < 0.05$) in up-regulation at least 2-fold in comparison to controls. Data are mean ± SEM of 3 experiments.

mechanically loaded spinal cord cells. MAPKs are a family of related serine/threonine protein kinases that transduce several signals responsible for cell proliferation or cellular stress, and are also intracellular signaling systems that induce optimal stress responses. In general, MAPK is activated by phosphorylation of tyrosine and threonine residues by MAPKK, which is activated through phosphorylation by MAPKKK. In KEGG analysis, the MAPK signaling pathway can be classified into three main groups [37]: the classical MAP pathway, the c-Jun N-terminal kinase or stress-activated protein kinase (JNK), the p38 MAPK signaling pathway, and the ERK pathway. In the present study, the mRNA expression levels of PDGFR and G12 significantly increased during the mid period of cyclic tensile stress application, while CACN, Raf1, MKP, JIP3, HSP72, GAD D45, and GAD D153 mRNA levels increased during the late phase of the cyclic tensile stress application. These genes, which were further identified by real time RT-PCR analysis, may play an important role in the response of spinal cord cells to neuronal injury. Previous *in vivo* studies of spinal cord injuries using microarray have also demonstrated the participation of similar genes in acute phage after injury [9,13]. Gene expression of trkA/B, FGFR, PDGFR, and Raf1 could

facilitate neuronal survival, while gene expression of G12, HSP72, GAD D45, GAD D153 could be involved in DNA damage. Further studies that target specific gene expression pathways will help determine their precise role in neuronal responses to mechanical load.

Our study is perhaps the first to attempt investigating the expression of genes related to apoptotic cell death during the application of cyclic tensile stress to neuronal rich spinal cord cells; however, it has several limitations. These include (i) imperfect validity of microarray results, with a CV of 5-15% for quantitative signals [38]; (ii) the neuronal culture was not 100% pure (the rate of NeuN-positive cells was 71%), and embryonic cells were used, not adults cells; and (iii) the lack of immunohistological or in situ hybridization data to identify the exact types of cells in which alterations in gene expression occurred. Nevertheless, we believe that the present study might be the first to comprehensively profile changes in gene expression involved in neuronal responses to cyclic tensile stress in cultured spinal cord cells using DNA microarray. This is a considerable improvement in examining the specific response of neuronal cells to mechanical load. Considered together with our previous findings [23], we can conclude that certain apoptosis-specific genes are activated in neuronal cell rich cultures during the application of cyclic tensile stress. The clinical relevance of tensile stress may specifically include the tethering effect with the developmental ascensus medullaris [23], cervical myelopathy in association with kyphotic deformity [4], and complicated spinal cord distraction injury. However, it is perhaps intuitive to consider that abnormal tensile stresses are involved in many mechanical insults of the spinal cord. Thus, we believe that our study provides new insights into the pathophysiology of spinal cord damage in various disease entities. Furthermore, the current study may help understand the response of neuronal cells to cyclic tensile stress and therapeutic issues related to the mechanically damaged spinal cord.

Conclusions

We have investigated the effects of cyclic tensile stresses on cultured spinal cord cells and demonstrate that cell death was induced depending on the level and duration of strain applied. Furthermore, we have performed a comprehensive analysis of alterations in gene expression profiles that occur following this mechanical stress, and identified in particular an upregulation of members of the MAPK pathway. Knowledge of the specific response of neuronal cells to mechanical insult could be a potentially useful tool for molecular-based therapy for spinal cord injury.

Methods

Cell isolation and culture

Primary cultures were established using the method described previously by our group [23]. In brief, the spinal cords of Sprague-Dawley rat embryos were dissected out at post-coital day 15 and stripped of the dorsal root ganglia and meninges. Dissected tissues were rinsed with cold Ca^{2+}- and Mg^{2+}-free Hanks balanced salt solution (HBSS) supplemented with 4 g/L glucose, and incubated at 37°C for 20 minutes with 0.03% (w/v) trypsin solution in HBSS under mild shaking. They were transferred into HBSS containing 0.1% (w/v) soyabean trypsin inhibitor (Sigma, St. Louis, MO) and 0.2% (w/v) bovine serum albumin (BSA), and triturated very mildly. The cell suspension was filtered through nylon mesh (70 μm, Cell Strainer; Becton Dickinson, Bedford, MA). The culture medium consisted of 75 mL Leibovitz's L-15 medium supplemented with glucose (4 g/L), 1.0 mL N2 supplement, 15 mL 0.15 M sodium bicarbonate, 10 mL heat-inactivated horse serum, 1 mL of 100 mM L-cysteine and 1 mL penicillin G 10^4 U/mL and neutralized with CO2. After centrifugation at 400 × g for 15 minutes at 4°C, the precipitated cells were gently re-suspended in a fresh culture medium and plated at a density of 4.0×10^5 cells/well onto a 6-well culture plate with a flexible-polystyrene bottom coated with type IV collagen (BioFlex® Baseplate, Flexercell International).

The experiment was carried out in the Orthopaedic Spinal Cord Laboratory of our University Medical Faculty. The experimental protocol strictly followed the Ethics Review Committee Guidelines for Animal Experimentation of our University.

Application of cyclic tensile stress to the cultured spinal cord cells

The cell stretching device used in this study was the Flexercell FX3000® (Flexercell International). The device consists of a computer-controlled vacuum unit, a culture plate with a flexible-polystyrene well-bottom coated with type IV collagen (BioFlex® Baseplate), and another culture plate with a non-deformable culture well bottom constructed of the same material as control. The culture plates consisted of 6-well (35 mm diameter) flexible-bottomed culture plate with a hydrophilic surface. The application of a vacuum provides a hemispherically downward deforming force onto the flexible bottom, resulting in a non-homogenous strain profile with a maximum at the periphery and a geometric decline toward zero at the center of the culture well bottom. For these experiments, the cultured spinal cord cells were subjected to various conditions. The flexible-bottomed culture plates including the control plates were then placed on the vacuum

baseplate in the incubator (37°C in 5% CO2). Three days after cell seeding, the cells were subjected to cyclic tensile stress for up to 72 hours. Previously we have documented [23] that ~71% of cells isolated from the spinal cord using this methodology are positive for the neuronal marker NeuN (Chemicon International, Temecula, CA). Repeated examinations by phase contrast microscopy showed that the cells remained attached to the substratum during elongation of the flexible-polystyrene well plates as tensile stresses were applied. Panjabi and White [16] demonstrated that the elastic properties of the cervical spinal cord are dramatically altered when it is subjected to approximately 10% elongation. In our previous *in vivo* study [17], the amplitude of epidurally-recorded spinal cord evoked potentials began to diminish, especially the second component (N2 spike), when the longitudinal extension of the cord shortened by 10-17%. Thus, in the present study, we set the tensile stress levels at a maximum 15% elongation and set the strain rate to estimate an appropriate frequency of spine movement in everyday life. Therefore, the cells were observed morphologically following application of various tensile stresses resulting in strains of 5%, 10%, and 15% applied at frequencies of 0.5 Hz and 1 Hz. Analyses of cell survival, DNA microarrays and real-time RT-PCR were conducted at 0, 2, 6, 12, 24, 48 and 72 hours after the application of the cyclic tensile load. DNA microarray analysis and real time RT-PCR were performed to compare the levels of gene expression at time 0 with levels of gene expression thereafter after the cyclic tensile loading at o.5 Hz, resulting in 10% strain.

Quantification of cell survival under cyclic tensile stress

Cell survival was investigated by scoring the number of living cells after tensile stress application using the Live/Dead Assay (Live/Dead Assay, Molecular Probes, Eugene, OR), according to the manufacturers' instruction. This assay if based on the differential staining of cells with calcein-acetoxymethyl ester (calcein AM: 3.00 μM) to identify living cells and ethidium homodimer-1 to identify dead cells [39,40]. Calcein-AM is a membrane-permeable dye that is cleaved by intracellular esterase to produce an impermeant green-wavelength fluorophore in living cells. Ethidium homodimer-1 cannot penetrate live cells, but it can enter dead cells which have a porous membrane and hence bind to DNA to produce red fluorescence. The culture medium was removed and the cells were then washed twice with PBS, and stained for 75 minutes at 32°C. The numbers of attached living cells (green) in at least 6 high-power fields (each containing at least 100 cells) were counted using fluoromicroscopy (IX70, Olympus, Tokyo) and a color image analyzer (MacSCOPE, Mitani, Fukui, Japan) in more than three wells for each time point. There was no evidence of spinal cord cell proliferation during the 3 day period prior to treatment with cyclic tensile stress, i.e. cell counts were almost uniform and at a density between 3.3×10^5 and 4.8×10^5 cells/well after dissemination on Bioflex® Baseplate in the absence of mechanical stimuli. The cell survival rate (%) at each time point for cultures which were subjected to 10% strain at 0.5 Hz frequency was calculated relative to the cell number at 0-hour. These cultures (subjected to 10% tensile strain at 0.5 Hz frequency) were then set as a standard, to which the cell viability of other levels of strain and frequency were compared.

All values were expressed as mean ± standard error of the mean (SEM). Differences between values of the loaded and control cultures were tested at each point by one-way ANOVA and Tukey posthoc test using the SPSS software version 11.0 (SPSS, Chicago, IL). P values of less than 0.05 denoted the presence of a statistically significant difference.

TEM examination

The presence of DNA fragmentation was examined via TEM examination. After application of tensile stresses, cultured spinal cord cells were washed twice with PBS and fixed with 2.5% glutaraldehyde and 2.5% paraformaldehyde, followed by late fixation in 1% osmium tetroxide for 2 hours. Fixed specimens were dehydrated in a graded series of alcohol, embedded in epoxy resin and polymerized at 60°C for 2 days. Ultrathin sections were cut by ultramicrotome, stained with uranyl acetate and lead citrate, and examined with a Hitachi H-7650 TEM (Hitachi, Tokyo).

RNA preparation and DNA microarray hybridization

The cultured cells on each well at 0, 2, 6, 12, 24, 48 and 72 hours were disrupted in a lysis buffer containing β-mercaptoethanol and the total RNA from five animals was pooled at each time point, and further purified using RNeasy® Mini Kit (Qiagen, Valencia, CA) and treated with DNase I (TaKaRa Bio, Ohtsu, Japan). The quality of RNA was initially assessed by electrophoresis on a 1.5% agarose gel, and further determined by using the RNA 6000 Nano LabChip Kit® and Agilent Bioanalyzer 2100 (Agilent, Palo Alto, CA). cDNAs were synthesized by GeneChip T7-Oligo (dT) Promoter Primer Kit® (Affymetrix, Santa Clara, CA) and TaKaRa cDNA Synthesis Kit® (TaKarRa Bio) from 3 μg total RNA. Biotinylated cRNA were synthesized using the IVT Labeling Kit (Affymetrix). Following fragmentation, 20 μg of cRNA were hybridized for 16 hours at 45°C on the GeneChip® Rat Genome 230 2.0 Array. GeneChips were washed and stained in the Affymetrix Fluidics Station 450, and scanned using GeneChip Scanner 3000 7G.

Data analysis of GeneChip® expression array

Microarray data was initially processed using GeneChip Operating Software (GCOS, Affymetrix). Signal intensity was calculated by Microarray Suite version 5.0 (MAS5.0) with Affymetrix default setting and global scaling as the normalization method. The trimmed mean target intensity of each array was arbitrarily set to 500. The ratio and difference of intensity between two corresponding genes on each array was calculated. Significance of the difference in levels of gene expression was set at a ratio and difference of intensity of ^2 and ^200, respectively. Spots that could not be interpreted were excluded, resulting in a list of 3,412 genes available for subsequent analysis. After filtering, the hierarchical clustering was applied to the axis using the complete linkage method, as implemented in the program Spotfire 8.1.1. The distance matrices used were uncentered, with correlation calculated on the basis of expression signals for clustered genes.

GO and KEGG analysis

We used the GO system and KEGG system for categorizing identified genes, and identified specific genes and pathways in each category by enrichment analysis. The Gene Ontology Consortium (http://www.geneontology.org/doc/GO.doc.html) maintains a controlled vocabulary database of functional descriptions for genes. These are divided into three families: biological process, cellular component, and molecular function. We searched for GO terms associated with Gene ID for GeneChip® Rat Genome 230 2.0 Array and were able to associate 3,540 of them with GO terms (GO numbers). In our study, we used the total list of GO terms within the biological process categories. The number of times a GO term (or group of terms) appeared at each sub-level of the GO tree was counted, and hierarchical sums were calculated (of the number of occurrences at or below each sub-branch). The KEGG system (http://www.genome.jp/kegg/) provides a reference knowledge base for linking genomes to life through the process of pathway mapping. We calculated a probability to determine whether any GO terms or pathways annotate a specified list of genes at a frequency greater than that would be expected by chance. The probability was determined using the following hypergeometric distribution formula:

$$P = 1 - \sum_{i=0}^{k-1} \frac{\binom{M}{i}\binom{N-M}{n-i}}{\binom{N}{i}}$$

where N is the total number of genes, M is the number of genes that annotated for a given term or pathway, n is the size of the list of genes of interest and k is the number of genes within the list that annotated for a given term or pathway.

Microarray including GeneChip® loads some different prove sequences in order to identify one gene. Strictly speaking, microarray data based on signal intensity represents the loading common probe set domain designed by Affymetrix. Therefore, it is possible that the number of gene symbols is different from that of the identified gene by the probe set.

Table 4: Sequences of primers used for real-time PCR

Target Protein	Forward Primer	Reverse Primer	PCR Product Size (bp)	Sequence Accession No.
CACN	5'-TCACCATTGCCTCCGAACACTA-3'	5'-CAGGAGCATTTCTGCCGTGA-3'	104	NM012517
TrkA/B	5'-GCCACACAATGTTGCCCATC-3'	5'-AAGGACTCTGCCCTGGGTGA-3'	185	NM012731
FGFR	5'-TTGCCGAATGAAGACCACGA-3'	5'-GGAGTTCATGGACGAGCTGGA-3'	130	NM001109892
PDGFR	5'-GAATGACCACGGCGATGAGA-3'	5'-GGATAAGCCTCAAACACCACCTG-3'	141	NM031525
G12	5'-CAAGATGCTGGTGGCTGTCAA-3'	5'-AGCAGCTCTGCCTCACGATG-3'	81	NM021589
Raf1	5'- AACAGTGAAGTCGCGCTGGA-3'	5'- CAGCACAATGCCATAGGAGTAGACA-3'	145	NM012639
MKP	5'-ACAACCACAAGGCAGACATTAGCTC-3'	5'- CAGATGGTGGCTGACCTGGA-3'	127	NM053769
JIP3	5'-AGCCTGCCTGCCAAGTACAAG-3'	5'-TCAGGTTGACACCAGCAGCAC-3'	148	NM001100673
HGK	5'-TTCACCATGTCATTCACCGAGA-3'	5'-CCAGCTGAGCGCTTACACCA-3'	99	NM001106904
HSP72	5'-GCTTTCACCTCAAGCCTTTGGA-3'	5'-CGGGCCTCATGCACACATAG-3'	117	NM212504
GAD D45	5'-AGGCAGCCAAGCTGCTCAA-3'	5'-ACGTCCCGGTCGTCATCTTC-3'	82	NM024127
GAD D153	5'-TGGAAGCCTGGTATGAGGATCTG-3'	5'-GAGGTGCTTGTGACCTCTGCTG-3'	175	NM024134
GAPDH	5'-GGCACAGTCAAGGCTGAGAATG-3'	5'-ATGGTGGTGAAGACGCCAGTA-3'	143	NM017008

Real-time RT-PCR analysis

Reverse transcription was performed using 500 ng of total RNA, AMV reverse transcriptase XL (TaKaRa Bio) and random primer. Real-time PCR was performed on the PRISM 7000 (ABI) system using 1 μl of the synthesized cDNA and SYBR Green PCR master mix (Applied Biosystems, Foster, CA). Table 4 lists the primer sequences used in the present study. The target genes were amplified and analyzed in triplicate using ABI Prism 7000 SDS Software (Applied Biosystems). The expression levels of target genes were normalized to that of glyceraldehyde-3-phosphate dehydrogenase (GAPDH) at each time interval, and the relative expression levels of target genes were calculated relative to that at 0 hour.

Competing interests

The authors declare that they have no competing interests.

Authors' contributions

KU and HB designed the study and drafted the manuscript. KU carried out all the experiments and performed the statistical analysis. HN and TH participated in the microarray analysis. TY, KC and SK participated in the experiments of cell morphology and viability. WEJ conceived the study, participated in its design and coordination and SR helped to draft the manuscript. All authors read and approved the final manuscript.

Acknowledgements

We are indebted to Yoshimasa Tsujimoto (Dragon Genomics Center, TAKARA BIO INC.) for support of analysis the data. This work was supported in part by Grants-in-Aid to HB, KU and HN for General Scientific Research of the Ministry of Education, Science and Culture of Japan (grants numbers 16390435, 18390411, 19791023, 21591895, 21791389, and 22390287). This work was also supported in part by grants from the Investigation Committees on Ossification of the Spinal ligaments (2005-2009) and Research Program of Spinal Cord Intractable Pain (2009), The Public Health Bureau of the Japanese Ministry of Health and Welfare.

Author Details

[1]Department of Orthopaedics and Rehabilitation Medicine, Fukui University Faculty of Medical Sciences, Shimoaizuki 23, Matsuoka, Fukui 910-1193, Japan and [2]Institute for Science & Technology in Medicine, Keele University at the RJAH Orthopaedic Hospital, Oswestry, Shropshire SY10 7AG, UK

Received: 7 December 2009 Accepted: 22 July 2010
Published: 22 July 2010

References

1. Baptiste DC, Fehling MG: **Pathophysiology of cervical myelopathy.** *Spine J* 2006, **6(6 Suppl)**:190S-197S.
2. Uchida K, Baba H, Maezawa Y, Furukawa S, Omiya M, Kokubo Y, Kubota C, Nakajima H: **Increased expression of neurotrophins and their receptors in the mechanically compressed spinal cord of the spinal hyperostotic mouse (*twy/twy*).** *Acta Neuropathol* 2003, **106**:29-36.
3. Ghafoor AU, Martin TW, Gopalakrishnan S, Viswamitra S: **Caring for the patients with cervical spine injuries: what have we learned?** *J Clin Anesth* 2005, **17**:640-649.
4. Uchida K, Nakajima H, Sato R, Yayama T, Erisa S, Mwaka ES, Kobayashi S, Baba Hisatoshi: **Cervical spondylotic myelopathy associated with kyphosis or sagittal sigmoid alignment: outcome after anterior or posterior decompression.** *J Neurosurg Spine* **11**:521-528.
5. Hayes RL, Yang K, Raghupathi R, McIntosh TK: **Changes in gene expression following traumatic brain injury in the rat.** *J Neurotrauma* 1995, **12**:779-790.
6. Raghupathi R, McIntosh TK: **Regionally and temporally distinct patterns of induction of c-fos, c-jun and junB mRNAs following experimental brain injury in the rat.** *Brain Res Mol Brain Res* 1996, **37**:134-144.
7. Sall JM, Morehead M, Murphy S, Goldman H, Walker PD: **Alterations in CNS gene expression in a rodent model of moderate traumatic brain injury complicated by acute alcohol intoxication.** *Exp Neurol* 1996, **139**:257-268.
8. Yakovlev AG, Faden AI: **Molecular biology of CNS injury.** *J Neurotrauma* 1995, **12**:767-777.
9. Carmel JB, Galante A, Soteropoulos P, Tolias P, Recce M, Young W, Hart RP: **Gene expression profiling of acute spinal cord injury reveals spreading inflammatory signals and neuron loss.** *Physiol Genomic* 2001, **7**:201-213.
10. Song G, Cechvala C, Resnick DK, Dempsey RJ, Rao VL: **GeneChip analysis after acute spinal cord injury in rat.** *J Neurochem* 2001, **79**:804-815.
11. Tachibana T, Noguchi K, Ruda MA: **Analysis of gene expression following spinal cord injury in rat using complementary DNA microarray.** *Neurosci Lett* 2002, **327**:133-137.
12. Aimone JB, Leasure JL, Perreau VM, Thallmair M: **Spatial and temporal gene expression profiling of the contused rat spinal cord.** *Exp Neurol* 2004, **189**:204-221.
13. Di Giovanni S, Knoblach SM, Brandoli C, Aden SA, Hoffman EP, Faden AI: **Gene profiling in spinal cord injury shows role of cell cycle in neuronal death.** *Ann Neurol* 2003, **53**:454-468.
14. Popovich PG, Strokes BT, Whitacre CC: **Concept of autoimmunity following spinal cord injury: possible roles for T lymphocytes in the traumatized central nerve system.** *J Neurosci Res* 1996, **45**:349-363.
15. Morrison B III, Saatman KE, Meaney DF, McIntosh TK: ***In vitro* central nervous system models of mechanically induced trauma. A review.** *J Neurotrauma* 1998, **15**:911-928.
16. Panjabi MM, White AA III: **Physical properties and functional biomechanics of the spine: the spinal cord.** In *Clinical Biomechanics of the Spine* 2nd edition. Edited by: White AA III, Panjabi MM. Philadelphia: J.B. Lippincott; 1996:67-71.
17. Kawahara N, Baba H, Nagata S, Kikuchi Y, Tomita K, Nomura S, Yugami H: **Experimental studies on the spinal cord evoked potentials in cervical spine distraction injuries.** In *Spinal Cord Monitoring and Electrodiagnosis* Edited by: Shimoji K, Kurokawa T, Tamaki T, Willis WD Jr. Tokyo: Springer-Verlag; 1991:107-115.
18. Bilston LE, Thibault LE: **The mechanical properties of the human cervical spinal cord in vitro.** *Ann Biomed Eng* 1996, **24**:67-74.
19. Shimizu K, Nakamura M, Nishikawa Y, Nishikawa Y, Hijikata S, Chiba K, Toyama Y: **Spinal kyphosis causes demyelination and neuronal loss in the spinal cord: a new model of kyphotic deformity using juvenile Japanese small game fowls.** *Spine* 2005, **30**:2388-2392.
20. Gilbert JA, Weinhold PS, Banes AJ, Link GW, Jones GL: **Strain profiles for circular cell culture plates containing flexible surfaces employed to mechanically deform cells *in vitro*.** *J Biomech* 1994, **27**:1169-1177.
21. Matsumoto T, Kawakami M, Kuribayashi K, Takenaka T, Tamaki T: **Cyclic mechanical stretch stress increases the growth rate and collagen synthesis of nucleus pulposus cells in vitro.** *Spine* 1999, **24**:315-319.
22. Nakatani T, Marui T, Hirota T, Doita M, Nishida K, Kurosaka M: **Mechanical stretching force promotes collagen synthesis by cultured cells from human ligamentum flavum via transforming growth factor-β1.** *J Orthop Res* 2002, **20**:1380-1386.
23. Uchida K, Nakajima H, Takamura T, Furukawa S, Kobayashi S, Yayama T, Baba H: **Gene expression profiles of neurotrophic factors in rat cultured spinal cord cells under cyclic tensile stress.** *Spine* 2008, **33**:2596-2604.
24. Morrison B III, Meaney DF, Margulies SS, McIntosh TK: **Dynamic mechanical stretch of organotypic brain slice cultures induces differential genomic expression: relationship to mechanical parameters.** *J Biomech Eng* 2000, **122**:224-230.
25. Haq F, Keith C, Zhang G: **Neurite development in PC12 cells on flexible micro-textured substrates under cyclic stretch.** *Biotechnol Prog* 2006, **22**:133-140.
26. Morrison B III, Cater HL, Wang CC, Thomas FC, Hung CT, Ateshian GA, Sundstrom LE: **A tissue level tolerance criterion for living brain developed with an in vitro model of traumatic mechanical loading.** *Stapp Car Crash J* 2003, **47**:93-105.
27. Tanoue M, Yamaga M, Ide J, Takagi K: **Acute stretching of peripheral nerves inhibits retrograde axonal transport.** *J Hand Surg [Br]* 1996, **21**:358-363.
28. Banes AJ, Tsuzaki M, Yamamoto J, Fischer T, Brigman B, Brown T, Miller L: **Mechanoreception at the cellular level; The detection, interpretation, and the diversity of responses to mechanical signals.** *Biochem Cell Biology* 1995, **73**:349-365.

29. Guharay F, Sachs F: **Stretch-activated single ion channel currents in tissue-cultured embryonic chick skeletal muscle.** *J Physiol* 1984, **352**:685-701.
30. Burridge K, Fath K, Kelly T, Nuckolls G, Turner C: **Focal adhesions: transmembrane junctions between the extracellular matrix and the cytoskeleton.** *Ann Rev Cell Biol* 1988, **4**:487-525.
31. Clark EA, Brugge JS: **Integrins and signal transduction pathways: the road taken.** *Science* 1995, **268**:233-239.
32. Shyy JY, Chien S: **Role of integrins in cellular responses to mechanical stress and adhesion.** *Curr Opin Cell Biol* 1997, **9**:707-713.
33. Li C, Hu Y, Mayr M, Xu Q: **Cyclic strain stress-induced mitogen-activated protein kinase (MAPK) phosphatase 1 expression in vascular smooth muscle cells is regulated by Ras/Rac-MAPK pathways.** *J Biol Chem* 1999, **274**:25273-25280.
34. Li C, Xu Q: **Mechanical stress-initiated signal transductions in vascular smooth muscle cells.** *Cell Signal* 2000, **12**:435-445.
35. Copland IB, Post M: **Stretch-activated signaling pathways responsible for early response gene expression in fetal lung epithelial cells.** *J Cell Physiol* 2007, **210**:133-143.
36. Resnick N, Collins T, Atkinson W, Bonthron DT, Dewey CF Jr, Gimbrone MA Jr: **Platelet-derived growth factor B chain promoter contains a cis-acting fluid shear-stress-responsive element.** *Proc Natl Acad Sci USA* 1993, **90**:4591-4595.
37. Davis RJ: **The mitogen-activated protein kinase signal transduction pathway.** *J Biol Chem* 1993, **268**:14553-14556.
38. Shi L, Reid LH, Jones WD, Shippy R, Warrington JA, Baker SC, Collins PJ, de Longueville F, Kawasaki ES, Lee KY, Luo Y, Sun YA, Willey JC, Setterquist RA, Fischer GM, Tong W, Dragan YP, Dix DJ, Frueh FW, Goodsaid FM, Herman D, Jensen RV, Johnson CD, Lobenhofer EK, Puri RK, Schrf U, Thierry-Mieg J, Wang C, Wilson M, Wolber PK, Zhang L, Amur S, Bao W, Barbacioru CC, Lucas AB, Bertholet V, Boysen C, Bromley B, Brown D, Brunner A, Canales R, Cao XM, Cebula TA, Chen JJ, Cheng J, Chu TM, Chudin E, Corson J, Corton JC, Croner LJ, Davies C, Davison TS, Delenstarr G, Deng X, Dorris D, Eklund AC, Fan XH, Fang H, Fulmer-Smentek S, Fuscoe JC, Gallagher K, Ge W, Guo L, Guo X, Hager J, Haje PK, Han J, Han T, Harbottle HC, Harris SC, Hatchwell E, Hauser CA, Hester S, Hong H, Hurban P, Jackson SA, Ji H, Knight CR, Kuo WP, LeClerc JE, Levy S, Li QZ, Liu C, Liu Y, Lombardi MJ, Ma Y, Magnuson SR, Maqsodi B, McDaniel T, Mei N, Myklebost O, Ning B, Novoradovskaya N, Orr MS, Osborn TW, Papallo A, Patterson TA, Perkins RG, Peters EH, Peterson R, Philips KL, Pine PS, Pusztai L, Qian F, Ren H, Rosen M, Rosenzweig BA, Samaha RR, Schena M, Schroth GP, Shchegrova S, Smith DD, Staedtler F, Su Z, Sun H, Szallasi Z, Tezak Z, Thierry-Mieg D, Thompson KL, Tikhonova I, Turpaz Y, Vallanat B, Van C, Walker SJ, Wang SJ, Wang Y, Wolfinger R, Wong A, Wu J, Xiao C, Xie Q, Xu J, Yang W, Zhang L, Zhong S, Zong Y, Slikker W Jr: **The MicroArray Quality Control (MAQC) project shows inter- and intraplatform reproducibility of gene expression measurements.** *Nat Biotechnol* 2006, **24**:1151-1161.
39. Takeno K, Kobayashi S, Negoro K, Uchida K, Miyazaki T, Yayama T, Shimada S, Baba H: **Physical limitations to tissue engineering of intervertebral disc cells: effect of extracellular osmotic change on glycosaminoglycan production and cell metabolism. Laboratory investigation.** *J Neurosurg Spine* 2007, **7**:637-644.
40. Vaughan PJ, Pike CJ, Cotman CW, Cunningham DD: **Thrombin receptor activation protects neurons and astrocytes from cell death produced by environmental insults.** *J Neurosci* 1995, **15**:5389-5401.

doi: 10.1186/1471-2202-11-84
Cite this article as: Uchida *et al.*, Microarray analysis of expression of cell death-associated genes in rat spinal cord cells exposed to cyclic tensile stresses in vitro *BMC Neuroscience* 2010, **11**:84

SPINE Volume 35, Number 5, pp 497–504

Targeted Retrograde Gene Delivery of Brain-Derived Neurotrophic Factor Suppresses Apoptosis of Neurons and Oligodendroglia After Spinal Cord Injury in Rats

Hideaki Nakajima, MD, PhD,* Kenzo Uchida, MD, PhD,* Takafumi Yayama, MD, PhD,* Shigeru Kobayashi, MD, PhD,* Alexander Rodriguez Guerrero, MD,* Shoei Furukawa, PhD,† and Hisatoshi Baba, MD, PhD*

Study Design. Histologic and immunohistochemical studies after targeted retrograde adenovirus (AdV)-mediated brain-derived neurotrophic factor (BDNF) gene delivery *via* intramuscular injection in rats with injured spinal cord.

Objective. To investigate the neuroprotective effect of targeted retrograde AdV-BDNF gene transfection in the traumatically injured spinal cord in terms of prevention of apoptosis of neurons and oligodendrocytes.

Summary of Background Data. Several studies investigated the neuroprotective effects of neurotrophins including BDNF on spinal cord injury, with respect to prevention of neural cell apoptosis in injured spinal cord. However, no report has described the potential effect of targeted retrograde neurotrophic factor gene delivery in injured spinal cord on prevention of neural cell apoptosis.

Methods. AdV-BDNF or AdV-LacZ was used for retrograde delivery *via* bilateral sternomastoid muscles to the spinal accessory motoneurons immediately after spinal cord injury in rats. Localization of β-galactosidase expression produced by LacZ gene or AdV-BDNF gene transfection was examined by immunofluorescence staining and double staining of cell markers (NeuN, RIP, GFAP, OX-42, and NG2) in the injured spinal cord. TUNEL-positive cells were counted and immunoreactivity to active caspase-3 and NG2 was examined after gene injection.

Results. Retrograde delivery of LacZ marker gene was identified in cervical spinal neurons and glial cells including oligodendrocytes in the white matter.

AdV-BDNF transfection resulted in a significant decrease in the number of TUNEL-positive apoptotic cells by downregulating the caspase apoptotic pathway, with significant promotion of NG2 expression in injured spinal cord, compared with AdV-LacZ injection.

Conclusion. Our results suggest that targeted retrograde BDNF gene delivery suppresses apoptosis of neurons and oligodendrocytes in the injured rat spinal cord.

Key words: brain-derived neurotrophic factor (BDNF), retrograde gene transfer, adenoviral vector (AdV), apoptosis, spinal cord injury. **Spine 2010;35:497–504**

Traumatic spinal cord injury can cause neural tissue damage, reduce neuronal cell survival activity including protein synthesis, necrosis and apoptosis. Several studies have demonstrated the rapid appearance of apoptotic neurons and glial cells in the injured cord segments and adjacent areas following spinal cord injury.[1–4] In addition to neuronal apoptosis, programmed cell death of oligodendrocytes was also observed along the longitudinal axis of the spinal cord, which could be involved in delayed and prolonged process of demyelination and deterioration of sensorimotor function of the cord.[3,5] Because prevention of apoptosis that occurs after spinal cord injury could potentially lead to spinal cord tissue restoration and motor function improvement, it has become a target for drug therapy. A number of clinical trials have reported success in suppressing apoptotic cell death after spinal cord injury.[6,7]

Neurotrophic factors are required for neuronal survival and influence axonal elongation during normal development.[8–10] Deficiency of endogenous neurotrophic factors is a serious problem for neuronal cell survival,[8,11] therefore, exogenous administration of neurotrophic factors has been proposed as one potential treatment for spinal cord injury.[12–14] Effective neurotrophin delivery promotes neuronal cell survival, prevent neuronal cell atrophy, and potentially facilitate axonal regeneration. In this context, targeted neurotrophin gene delivery through peripheral nerves or target muscle transmitted by adenoviral vectors (AdV) is less invasive with the potential of repeated administration,[15,16] compared with direct administration of gene transduction to the nervous system by intrathecal, intracerebroventricular, or intraparenchymal infusion.[17] Such retrograde approach has been used for gene delivery to the central nervous system including the spinal cord.[9,10,18–20] Our group has also reported the feasibility of retrograde delivery of adenovirus genome to the cervical and lumbar segments through injection of an adenovirus vector into the target muscles using AdV carrying β-galactosidase (AdV-LacZ)

From the *Department of Orthopaedics and Rehabilitation Medicine, The University of Fukui, Fukui, Japan; and †Laboratory of Molecular Biology, Gifu Pharmaceutical University, Mitahora-higashi, Gifu, Japan.

Acknowledgment date: April, 4, 2009. Acceptance date: June 2, 2009. The manuscript submitted does not contain information about medical device(s)/drug(s).

Funds were received in support of this work. No benefits in any form have been or will be received from a commercial party related directly or indirectly to the subject of this manuscript.

Supported, in part, by Grant-in-Aid to HB, HN and KU for General Scientific Research of the Ministry of Education, Science and Culture of Japan (grants numbers C-15591571, B-16390435, B-18390411, and B-19791023), and by grants from the Investigation Committee on Ossification of the Spinal ligaments, the Public Health Bureau of the Japanese Ministry of Labor, Health and Welfare (2005–2008) (to H.B.).

Address correspondence and reprint requests to Hideaki Nakajima, MD, PhD, Department of Orthopaedics and Rehabilitation Medicine, The University of Fukui, Matsuoka Shimoaizuki 23–3, Eiheiji, Fukui 910-1193, Japan; E-mail: nhideaki@u-fukui.ac.jp

gene.[21,22] In the spinal hyperostotic mouse (*twy/twy*), our group has confirmed that AdV-mediated brain-derived neurotrophic factor (BDNF) gene *via* retrograde axonoplasmic transport could be transfected into cervical spinal cord neurons and some glial cells.[23]

However, it is not clear whether the AdV-BDNF suppresses neuronal and glial cell apoptosis in the acute spinal cord injury model, and there is no report that describes cell death, particularly apoptosis, following retrograde neurotrophin gene transfection. The present study was designed to investigate the effects of retrograde AdV-BDNF gene delivery on apoptosis of neurons and glial cells (oligodendrocytes) after traumatic spinal cord injury.

■ Materials and Methods

Production of Adenoviral Vector

AdV vectors-mediated BDNF was prepared using the instruction provided with the Adenovirus Expression Vector Kit (Takara Biomedicals, Ohtsu, Japan). The mouse BDNF cDNA was synthesized and confirmed, then subcloned into a cassette cosmid pAxCAwt carrying an adenovirus type-5 genome lacking the E3, E1A, and E1B regions. The cosmid pAxCAwt contains a *Swa*I cloning site flanked by a cytomegalovirus enhancer-chicken β-actin hybrid promoter on the 5′ end and a rabbit globulin poly(A) sequence on the 3′ end. The cosmid was co-transfected into 293 cells with the appropriately cleaved adenovirus DNA-terminal protein complex (COS-TPC method).[24] The recombinant adenovirus was propagated and isolated from 293 cells and purified using 2 rounds of CsCl centrifugation (AdV-BDNF). As a control maker gene, a recombinant adenovirus vector coding for bacterial β-galactosidase cDNA, was isolated using the same procedure (AdV-LacZ). The final titers of the adenovirus vector contained 5.0×10^8 plaque forming units/mL.

Animal Model of Spinal Cord Injury and Targeted AdV-BDNF Gene Delivery

The experimental protocol was approved by the Ethics Committee for Animal Experimentation of Fukui University. Experiments were conducted in 69 adult male Sprague-Dawley rats (Clea, Tokyo), aged 8 to 10 weeks with a mean body weight of 263 ± 27.6 g (±SD). Following anesthesia by intraperitoneal injection of sodium pentobarbiturate (0.05 mg/g body weight), laminectomy was performed at the C3 and C4 levels under a surgical microscope (VANOX-S, Olymus, Tokyo), taking utmost care in avoiding dura matter laceration. At the C4 vertebral level (C5 cord segment), the dorsal dural surface of the spinal cord was compressed extradurally using a 50 g static load (custom-made rod, 2 × 3 mm in diameter) for 5 minutes, as we described previously.[21,25] Immediately after the injury, the sternomastoid muscles were exposed on both sides while the rat was positioned in supine position using a stereotaxic surgical frame, taking utmost care in preserving branches of the spinal accessory nerves that innervate the muscles. Using a microsyringe (Hamilton, Reno, NV), each 100 μL of adenoviral vector encoding LacZ (5.0×10^8 PFU, n = 37) or BDNF (5.0×10^8 PFU, n = 23) was injected carefully and slowly into the middle belly of the superficial layer of the bilateral sternomastoid muscles simultaneously. AdV-LacZ injection without spinal cord injury (only operation for laminectomy) was used as normal groups (*i.e.*, positive controls; n = 9). The rat was then allowed to recover from anesthesia and housed under a 12- to 12-hour light-dark cycle in a bacteria-free bio-clean room with access to water and food *ad libitum*.

Immunohistochemistry, Double Staining, and Terminal Deoxynucleotidyl Transferase (TdT)-Mediated dUTP-Biotin Nick End Labeling (TUNEL) Staining

Following retrograde injection of AdV-LacZ or AdV-BDNF, the rat cervical spinal cord was perfused and fixed with 4% paraformaldehyde in 0.1 M phosphate-buffered saline (PBS) and postfixed in the same fixative (24 hours), 10% sucrose in 0.1 M PBS (24 hours), and 30% sucrose in 0.1 M PBS (24 hours). Segments of the spinal cord (between the pyramidal decussation and C7 segment) were embedded in optimal cutting temperature compound and cut on a cryostat into serial 25-μm thick transverse frozen sections (n = 53). The length from the caudal site to the rostral site of the spinal cord assessed histologically was on average 20 mm. For immunofluorescence staining, the sections were incubated at 4°C with polyclonal anti-β-galactosidase polyclonal antibody (1:10,000, rabbit IgG, Abcam plc, Cambridge, UK), antiactive caspase-3 polyclonal antibody (1:200, rabbit IgG; Abcam plc) diluted in antibody diluent with Background Reducing Components (Dako Cytomation, Carpentaria, CA). In the next step, the section were incubated with the secondary antibody, goat antirabbit Alexa Flour 488/fluorescein-conjugated antibody (1: 250; Molecular Probes, Eugene, OR), for 1 hour at room temperature. They were then incubated with antineuronal nuclei (NeuN) monoclonal antibody (1:400, mouse IgG; Chemicon International, Temecula, CA) for neurons, antireactive immunology protein (RIP) monoclonal antibody (1: 100,000, mouse IgG; Chemicon International) as a mature oligodendrocyte-specific marker, anti-NG2 monoclonal antibodies (1: 400, mouse IgG; Chemicon International) for chondroitin sulfate proteoglycan for oligodendroglial progenitor, antiglial fibrillary acidic protein (GFAP) monoclonal antibody (1:400, mouse IgG; Chemicon International) for astrocytes, and antimicroglia monoclonal antibody (OX42, CD11b, 1:400, mouse IgG; Abcam plc) for microglia, followed by goat antimouse Alexa Flour 568/fluorescein-conjugated antibody (1: 250; Molecular Probes).

DNA fragmentation was detected by the TUNEL method using ApopTag Plus Fluorescein *In Situ* Apoptosis Detection kit (Chemicon International) and the instructions provided in the kit manual. The reaction with TdT was terminated by washing the sections with a stop-wash buffer for 2 hours at 37°C. Antidigoxigenin-fluorescein was applied for 30 minutes at room temperature. All images were obtained using a fluorescence microscope (Olympus AX80, Olympus Optical, Tokyo) or a confocal laser scanning microscope (model TCS SP2, Leica Instruments, Nusslosh, Germany). Some sections were counterstained with nuclear marker DAPI (Abbott Molecular, Des Plaines, IL).

Luxol fast blue staining was properly performed to evaluate the gross morphology and the proportions of normal (n = 2) and injured (n = 2) spinal cords by axial sections. Gross assessment of localization of immunostained cells throughout the cephalocaudal direction (C0–C8 cord segments) was performed using sagittal sections (n = 12).

Immunoblot Analysis

Cervical spinal cord segments (10-mm long) centered around the site of injury (epicenter) were obtained after retrograde injection of AdV-LacZ (n = 2) or AdV-BDNF (n = 2) and

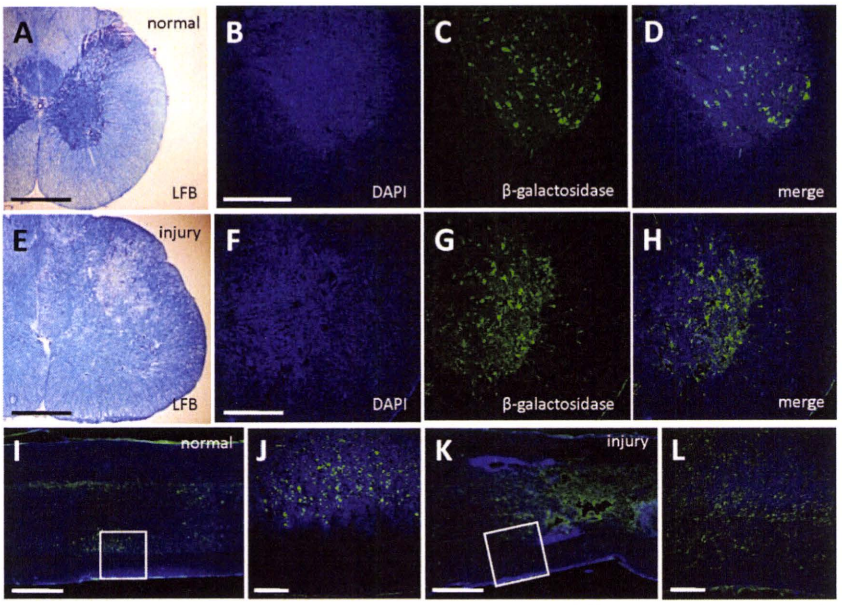

Figure 1. Photomicrographs showing immunofluorescence for β-galactosidase in axial and sagittal sections of normal (**A–D** and **I, J**) and injured (**E–H** and **K, L**) spinal cord at 1 week after AdV-LacZ gene injection. **A, E,** Luxol fast blue (LFB) staining. **B, F,** DAPI. **C, G,** β-galactosidase. **D, H–L,** Merged. Scale bar = 500 μm (**A, B, E, F**), 1 mm (**I, K**), 100 μm (**J, L**).

stored in liquid nitrogen. The samples were solubilized in RIPA buffer (50 mmol/L TRIS-HCl, pH 7.5, 150 mmol/L NaCl, 1% Triton X-100, 0.5% sodium deoxycholate, 20 μg/mL leupeptine, and 1 mmol/L phenylmethylsulfonylfluoride), homogenized and then stored at −80°C. The protein concentration was analyzed by Bio-Rad DC protein assay kit (No. 500–0116, Bio-Rad Laboratories, Hercules, CA). Laemmli sodium dodecylsulphate buffer samples containing proteins were boiled and subjected to immunoblot analysis. Total protein (80 μg/lane) was subjected to sodium dodecylsulphate polyacrylamide gel (15%) electrophoresis (SDS-PAGE) and transferred onto polyvinylidene difluoride membrane (PE Applied Biosystems, Foster, CA) for 70 minutes in a semidry blot apparatus. The membranes were then washed twice in PBS containing 0.05% Tween 20, and then blocked with 5% skim milk for 1 hour, subsequently reacted with antiactive caspase-3 polyclonal antibody (1:20, rabbit IgG; Abcam plc) diluted overnight at 4°C sequentially by antirabbit IgG antibody and avidin-biotinylated peroxidase complex (1:200; Envision System-HRP Labeled Polymer, Dako Cytomation) for 3 hours. After triple washing in PBS, the membrane was sunk in the enhanced chemiluminescence (ECL) for 1 minute to take an radiograph film for visualization of peroxidase activity.

Quantitative and Statistical Analyses

To quantify the TUNEL-positive and NG2-positive areas, images of transaxial sections were obtained. Six cross-sections were randomly selected out of 10 to 15 sections from 3 segments (site 5 mm rostral to the epicenter, site of epicenter at compression, and 5 mm caudal site distal to the epicenter) of each AdV-injected animal. TUNEL-positive and NG-2-positive areas (×10) in each immunofluorescence staining were analyzed using grain counting with the light intensity automatically by a color image analyzer (MacSCOPE, Mitani, Fukui, Japan).

The Mann-Whitney *U* test was used to compare the immunoreactive areas in each region between AdV-LacZ injected and AdV-BDNF injected animals. All values were expressed as mean ± SD. A *P* value <0.05 denoted the presence of a significant difference between groups.

■ Results

Distribution of β-Galactosidase Expression in the Spinal Cord by Retrograde Gene Delivery

To assess the distribution of β-galactosidase following retrograde gene delivery into the normal (Figure 1A) and injured (Figure 1E) spinal cord, immunofluorescence staining was performed and evaluated. β-galactosidase-positive cells were observed mainly in the gray matter including motoneurons and interneurons in the normal spinal cord on axial (Figures 1B–D) and sagittal sections (Figures 1I, J) of positive controls, while they were observed in all (gray matter and white matter) of the injured spinal cord on axial (Figures 1F–H) and sagittal (Figures 1K, L) sections. In injured spinal cord, double-stained cells for NeuN in gray matter, and RIP, GFAP, and OX-42 in white matter, with β-galactosidase, were clearly identified (Figure 2).

Apoptosis of Neurons and Oligodendrocytes

Histologic evaluation and immunoblot analysis were applied to assess the effects of retrograde BDNF gene delivery on apoptotic cell death in the injured spinal cord. A number of TUNEL-positive cells were found in both gray and white matters of the cord after AdV-LacZ gene transfection (Figure 3A). In comparison, TUNEL-positive cells were markedly decreased in the injured cord after treatment with AdV-BDNF gene transfection (Figure 3B). The number of TUNEL-positive cells per cross section significantly decreased in the AdV-BDNF injected group compared with the AdV-LacZ injected group at 3 days, 1 and 2 weeks after injury in the rostral and caudal adjacent site (Figures 3C, E), and at 1 week after the injury in the epicenter (Figure 3D). In the AdV-BDNF injected rats with cord contusion injury, fewer TUNEL-positive neurons and oligodendrocytes were found compared with AdV-LacZ transfection (Figure 4).

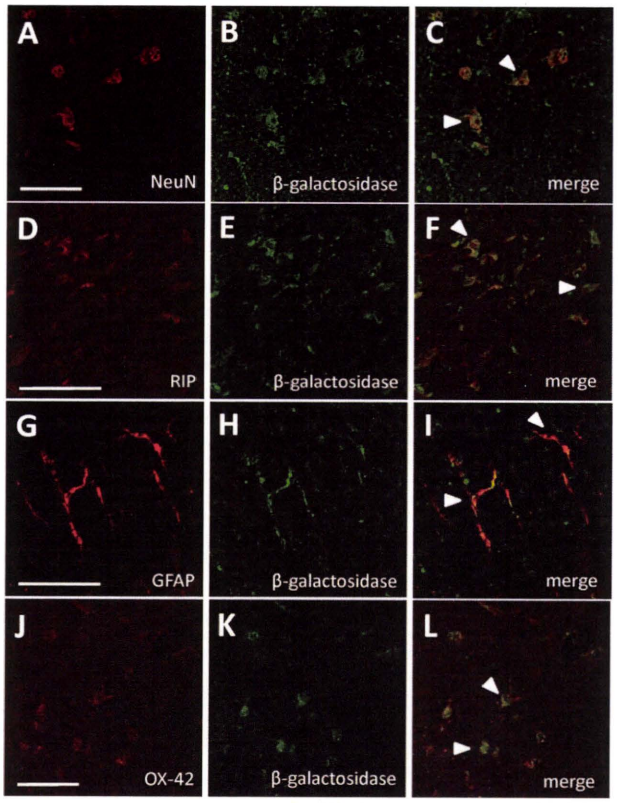

Figure 2. Colocalization of cell specific markers (red, left column; **A,** NeuN, **D,** RIP, **G,** GFAP, **J,** OX-42) and β-galactosidase (green, middle column; **B, E, H, K**) in the rat 1 week after spinal cord injury. Expression of β-galactosidase was confirmed in neurons, oligodendrocytes, astrocytes, and microglia, as appreciated in the merged images (**C, F, I, L**) following retrograde transfection of AdV-LacZ gene. Arrows indicate colocalization of β-galactosidase and each cell specific marker. Bar = 100 μm.

Figure 5 shows the results of immunoblot analysis and double immunofluorescence staining carried out to investigate the effect of retrograde gene transfection on the expression of active caspase-3. Immunoblot analysis of active caspase-3 showed intense molecular bands of 17.0 kDa. A band of active caspase-3 was evident from 3 hours to 1 week after spinal cord injury in AdV-LacZ treated rats, while the band appeared 3 to 12 hours later in AdV-BDNF gene injected animals (Figure 5A). Furthermore, expression of active caspase-3 was decrease in both neurons and oligodendrocytes after AdV-BDNF gene transfection (Figures 5B–E).

Effects of Retrograde AdV-BDNF Gene Delivery on Endogenous Oligodendrocyte Progenitor Cells

Expression of NG2 (precursor of oligodendrocyte lineage) in the white matter of the cord was investigated at 4 weeks after retrograde injection of AdV-BDNF. Abundant NG2-positive cells were noted in the white matter of AdV-BDNF- than AdV-LacZ-injected rats in transaxial (Figures 6A, B) sections. Quantitative analysis of NG2-positive area in AdV-BDNF-treated rats showed significant increase in all 3 anatomic sites (Figure 6C).

■ Discussion

A number of experimental studies and transduction approaches have attempted to establish feasible methods for improvement of neural function after spinal cord injury. These include stem cell replacement,[26] suppression of various inhibitory factors,[27] and neuronal progenitor cell induction and regeneration.[28] The delivery of neuroprotective genes such as neurotrophic factors can be potentially beneficial for restoration of neural tissue function after spinal cord injury.[9,10,13,16] Development of virus vector for gene delivery is a practically feasible tool for transduction of neurotrophic peptides.[29] However, effective administration of neuroprotective genes into the injured site of the cord remains a major challenge. Direct routes for administration of neuroprotective genes have been used for gene delivery. However, there are difficulties and serious concerns regarding the possible spread of traumatic neural injury and worsening of neural injury, including necrosis, and apoptosis as well as cell death.[30] In contrast, targeted retrograde gene delivery through

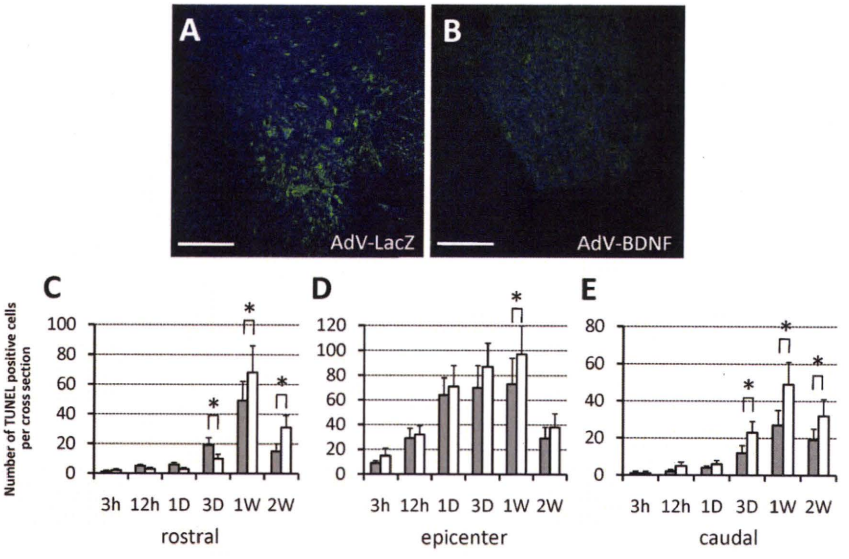

Figure 3. Photomicrographs showing TUNEL immunofluorescence staining in the injured spinal cord treated with AdV-LacZ (**A**) and AdV-BDNF (**B**). Bar = 500 μm. Bar graphs show results of quantitative analysis of TUNEL-positive cells per cross section following AdV-LacZ or AdV-BDNF transfection at rostral (**C**), epicenter (**D**), and caudal (**E**) sites of the injured cervical cord. Data are mean ± SD. *$P < 0.05$.

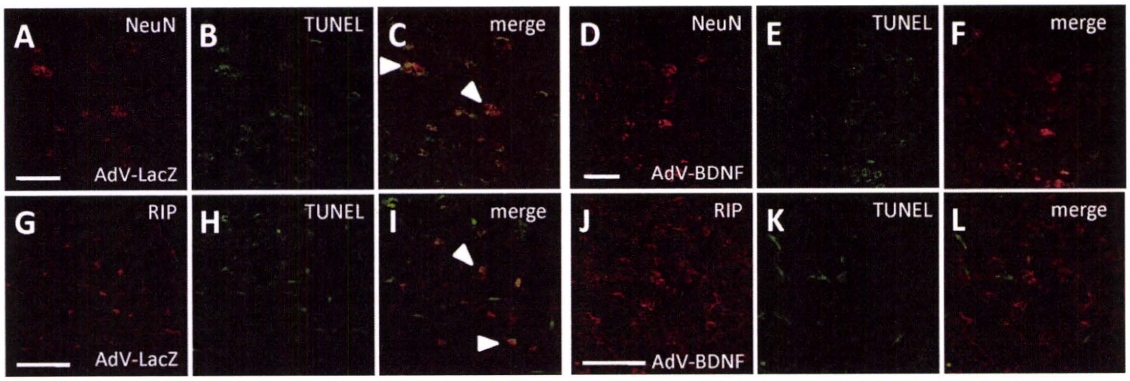

Figure 4. Top row: Photomicrographs of cells stained for NeuN, TUNEL, and NeuN/TUNEL following AdV-LacZ (**A–C**) or AdV-BDNF (**D–F**) gene transfection. Bottom row: Photomicrographs of cells stained for RIP, TUNEL, and RIP/TUNEL- double following AdV-LacZ (**G–I**) or AdV-BDNF (**J–L**) gene transfection. Bar = 100 μm (**A–F**), 50 μm (**G–L**).

the peripheral nervous system or by muscle injection of adenovirus vectors seems a less invasive method that can be conducted repeatedly.[16]

In a series of experiments, our group evaluated the feasibility and efficacy of retrograde gene delivery into the injured cervical spinal cord using recombinant adenovirus vector through the sternomastoid muscle, which is innervated by the spinal accessory nerve,[21,22] applying modified wheat germ agglutinin-horseradish peroxidase labeling method of cervical motoneurons pool.[9] β-galactosidase (AdV-LacZ) gene expression was found in the cervical spinal cord from 4 to 6 weeks after injection of adenovirus vector, reaching peak expression level at 1 to 2 weeks, and exhibiting transduction efficacy (survival rate of cervical spinal cord motoneurons: 87.5% to 98.9% within 3 days after injection).[21,22] Transduction of interneurons and glial cells (microglia, reactive astrocytes, and oligodendrocytes) induced by primary or secondary wave of injury could be verified with X-gal staining at early time after the trauma. Several investigators have reported cell proliferation and differentiation of glial progenitor cells in the residual white matter following spinal cord injury.[31–33] These surviving cells require neurotrophins even during the pathologic process after the trauma. The efficiency of retrograde delivery of neuropeptide genes could be influenced by various factors,[34] but our group has confirmed that AdV-LacZ is transported *via* retrograde axonoplasmic flow rather than through systemic circulation because no gene expression was observed in various peripheral organs.[22] Accordingly, targeted retrograde AdV-LacZ gene and hopefully AdV-BDNF gene delivery is considered feasible from a methodologic point of view.

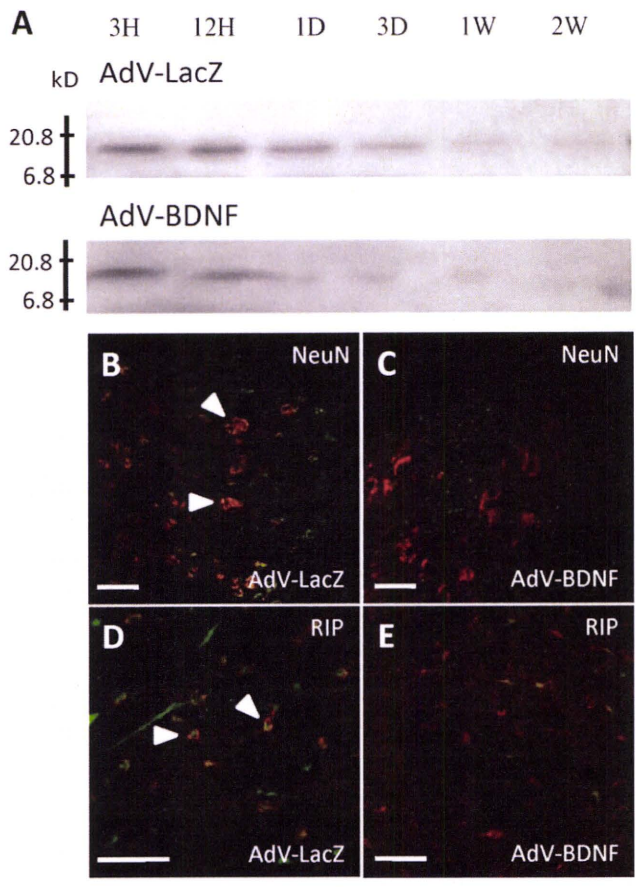

Figure 5. Immunoblot analysis for the expression of active caspase-3 (**A**) following AdV-LacZ or AdV-BDNF gene transfection into the injured cervical cord (top panels). Bottom panel: Photomicrographs showing double immunofluorescence staining for active caspase-3/NeuN (**B, C**), active caspase-3/RIP (**D, E**) 1 day after the spinal cord injury with AdV-LacZ (**B, D**) or AdV-BDNF (**C, E**) gene transfection. Bar = 100 μm (**B, C**), 50 μm (**D, E**).

Exogenous administration of BDNF promotes neural cell survival, alleviates neuronal atrophy,[13] facilitates axonal regeneration,[35] prevents apoptosis,[36,37] enhances differentiation of neuronal stem cells to neurons followed by improvement of motor function,[14] and induces glial cell proliferation, axonal outgrowth and myelination.[38] Our group has reported that retrograde AdV-BDNF gene transduction in the injured cervical cord plays a positive role in maintaining surviving neurons following trauma,[39] but there was no evidence of whether the same treatment suppressed neuronal and glial cell apoptosis. Previous studies reported that spinal cord injury resulted in induction of apoptosis mediated by caspase-3[40] and overexpression of the death receptors, especially Fas,[41] $p75^{NTR}$ peptide,[42] and mitogen-activated protein kinase (MAPK) pathway including

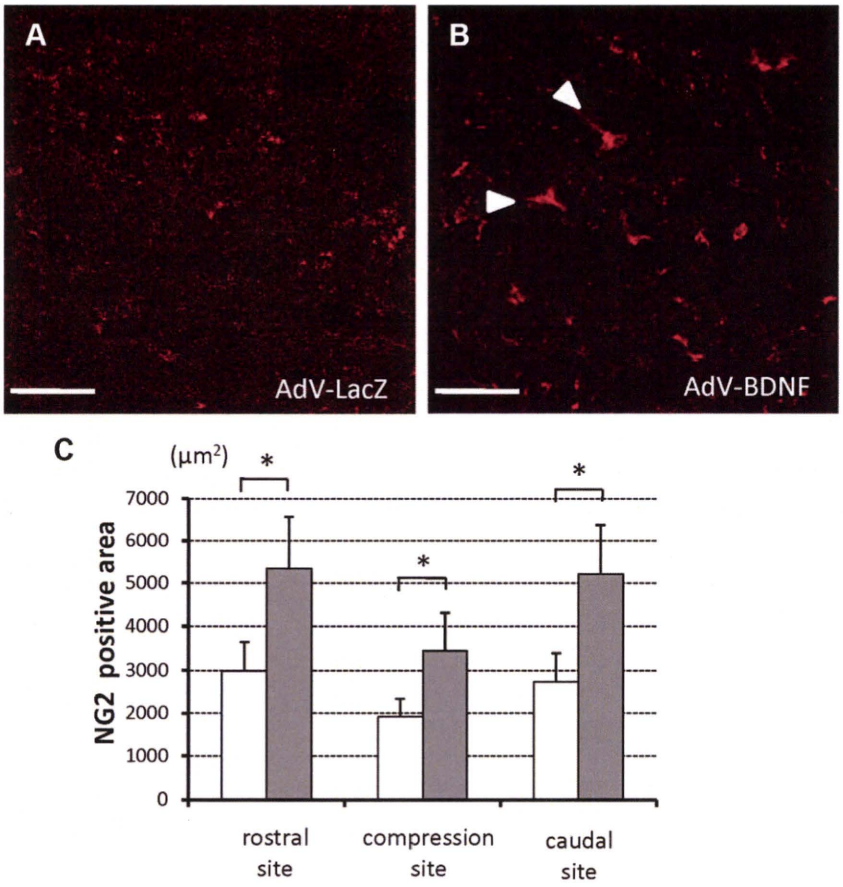

Figure 6. Photomicrographs showing the expression of NG2 in the white matter of injured spinal cord after AdV-LacZ (**A**) or AdV-BDNF (**B**) gene transfection. Transaxial sections of the cord show increased number of NG2-positive cells and area following AdV-BDNF gene transfection (**B** in comparison to **A**). Quantitative analysis of the NG2-positive area in the axial sections showed a significant increase of NG2 expression after AdV-BDNF gene injection (**C**). Data are mean ± SD. $*P < 0.05$. Bar = 50 μm (**A, B**).

apoptosis signal-regulating kinase 1 (ASK1), Jun N-terminal kinase (JNK), and p38 MAPK cascade.[4] Caspases are a family of cysteine proteases that play important roles in the effector phase of apoptosis and are activated through intrinsic and extrinsic pathways. Apoptosis of neurons and oligodendrocytes involves the activation of casepase-3.[43] Activation of casepase-3 and upregulation of these caspase mRNA levels occur immediately after spinal cord trauma.[44,45] Underexpression of these neuropeptides suggest suppression of neural cell apoptosis. Although TUNEL staining is not specific to apoptotic cells,[37] the retrograde delivery of AdV-BDNF to the epicenter and around injured site resulted in a significant decrease in the number of TUNEL-positive cells at early stage following traumatic cord injury, suggesting antiapoptotic effect of the treatment. Our observation also suggest that AdV-BDNF transduction immediately after the injury is attributable to downregulation of caspase-3-mediated pathway, particularly neurons and oligodendrocytes in animals with injured cervical spinal cord.

Oligodendrocytes that survive even under demyelinating injury to the cord were believed to be uncorrelated to remyelination.[46] Instead, the presence of NG2-labeled endogenous oligodendrocyte progenitor cells in the lesion indicates the proliferation of cycling cells,[47] and considered to contribute to myelin repair.[48] After spinal cord injury, expression and localization of NG2 were identified in the residual white matter,[33] and in the present study, they were also found in the traumatised and adjacent sites. While the issue of whether BDNF attenuates apoptosis of oligodendrocytes or not remains unresolved, oligodendrocytes express the full-length form of trkB, and their survival depends on the MAPK signaling pathway downstream of trkB.[49] In the present study, we found increased NG2 immunoreactivity after AdV-BDNF gene injection and potential antiapoptotic effect of BDNF that is conveyed to the neural cells *via* axonoplasmic transport. BDNF is reported to induce proliferation of oligodendrocytes and myelination of regenerating axons after spinal cord injury.[50] Accordingly, it is conceivable that increased the NG2 immunoreactivity following AdV-BDNF gene transfection represents antiapoptotic effect on neural cells including oligodendrocytes.

■ Conclusion

In conclusion, we have described the potential roles of targeted retrograde AdV-BDNF gene transfection to the traumatically injured cervical spinal cord in terms of significant reduction in the number of TUNEL-positive neurons and oligodendroglia. This action seems to be mediated by downregulation of caspase-3-mediated apoptotic cascade. Retrograde BDNF gene delivery is a potentially feasible method to promote the survival of

neurons and oligodendroglia after traumatic spinal cord injury.

■ Key Points

- Retrograde delivery of control LacZ marker gene *via* bilateral sternomastoid muscles to the cervical spinal cord was successfully transfected into neurons and glial cells including oligodendrocytes in and around injured site in rat spinal cord injury.
- Targeted retrograde delivery of AdV-BDNF gene to the epicenter and around the cord injured site resulted in a significant decrease in the number of TUNEL-positive apoptotic cells by downregulating the casepase-3 apoptotic pathway at early stage after the injury.
- Targeted delivery of AdV-BDNF gene increased endogenous NG2-labeled oligodendrocyte progenitor cells at 4 weeks.
- Targeted retrograde AdV-BDNF gene delivery is considered a potentially useful therapeutic tool for neuronal and oligodendrocyte survival after spinal cord injury.

References

1. Katoh K, Ikata T, Katoh S, et al. Induction and its spread of apoptosis in rat spinal cord after mechanical trauma. *Neurosci Lett* 1996;216:9–12.
2. Li GL, Brodin G, Farooque M, et al. Apoptosis and expression of bcl-2 after compression trauma to rat spinal cord. *J Neuropathol Exp Neurol* 1996;55:280–9.
3. Crowe MJ, Bresnahan JC, Shuman SL, et al. Apoptosis and delayed degeneration after spinal cord injury in rats and monkeys. *Nat Med* 1997;3:73–6.
4. Nakahara S, Yone K, Sakou T, et al. Induction of apoptosis signal regulating kinase 1 (ASK1) after spinal cord injury in rats: possible involvement of ASK1-JNK and p38 pathways in neuronal apoptosis. *J Neuropathol Exp Neurol* 1999;58:442–50.
5. Abe Y, Yamamoto T, Sugiyama Y, et al. Apoptotic cells associated with Wallerian degeneration after experimental spinal cord injury: a possible mechanism of oligodendroglial death. *J Neurotrauma* 1999;16:946–52.
6. Ray SK, Wilford GG, Matzelle DC, et al. Calpetin and methypredonisolone inhibit apoptosis in rat spinal cord injury. *Ann N Y Acad Sci* 1999;860:261–9.
7. Wada S, Yone K, Ishidou Y, et al. Apoptosis following spinal cord injury in rats and preventive effect of N-methyl-D-aspartate receptor antagonist. *J Neurosurg* 1999;91:98–104.
8. Bregman BS. Transplants and neurotrophins modify the response of developing and mature CNS neurons to spinal cord injury. Axonal regeneration and recovery of function. In: Kalb RG, Strittmatter SM, eds. *Neurobiology of Spinal Cord Injury*. Totowa, NJ: Humana Press; 2000:169–94.
9. Uchida K, Baba H, Maezawa Y, et al. Histological investigation of spinal cord lesions in the spinal hyperostotic mouse (*twy/twy*): morphological changes in anterior horn cells and immunoreactivity to neurotrophic factors. *J Neurol* 1998;245:781–93.
10. Uchida K, Nakajima H, Inukai T, et al. Adenovirus-mediated transfer of neurotrophin-3 gene enhances survival of anterior horn neurons of *twy/twy* mice with chronic mechanical compression of the spinal cord. *J Neurosci Res* 2008;86:1789–800.
11. Nakamura M, Bregman BS. Differences in neurotrophic factor gene expression profiles between neonate and adult rat spinal cord after injury. *Exp Neurol* 2001;169:407–15.
12. Kobayashi NR, Fan DP, Giehl KM, et al. BDNF and NT-4/5 prevent atrophy of rat rubrospinal neurons after cervical axonotomy, stimulate GAP-43 and Talphal-tubulin mRNA expression, and promote axonal regeneration. *J Neurosci* 1997;17:9583–95.
13. Novikova LN, Novikov LN, Kellerth JO. Survival effects of BDNF and NT-3 on axonotomized rubrospinal neurons depends on the temporal pattern of neurotrophin administration. *Eur J Neurosci* 2000;12:776–80.
14. Blits B, Boer GJ, Verhaagen J. Pharmacological, cell, and gene therapy strategies to promote spinal cord regeneration. *Cell Transplant* 2002;11:593–613.
15. Ruitenberg MJ, Eggers R, Boer GJ, et al. Adeno-associated viral vectors as agents for gene delivery: application in disorders and trauma of the central nervous system. *Methods* 2002;28:182–94.
16. Hendriks WT, Ruitenberg MJ, Blits B, et al. Viral vector-mediated gene transfer of neurotrophins to promote regeneration of the injured spinal cord. *Prog Brain Res* 2004;146:451–76.
17. Mannes AJ, Caudle RM, O'Connell BC, et al. Adenoviral gene transfer to spinal-cord neurons: intrathecal vs. intraparenchymal administration. *Brain Res* 1998;793:1–6.
18. Baumgartner BJ, Shine HD. Neuroprotection of the spinal motoneurons following targeted transduction with an adenoviral vector carrying gene for glial cell line-derived neurotrophic factor. *Exp Neurol* 1998;153:102–12.
19. Watabe K, Ohashi T, Sakamoto T, et al. Rescue of lesioned adult rat spinal motoneurons by adenoviral gene transfer of glial cell line-derived neurotrophic factor. *J Neurosci Res* 2000;60:511–9.
20. Sakamoto T, Kawazoe Y, Shen JS, et al. Adenoviral gene transfer of GDNF, BDNF, and TGF beta 2, but not CNTF, cardiotrophin-1 or IGF1, protects injured adult motoneurons after facial nerve avulsion. *J Neurosci Res* 2003;72:54–64.
21. Nakajima H, Uchida K, Kobayashi S, et al. Targeted retrograde gene delivery into the injured cervical spinal cord using recombinant adenovirus vector. *Neurosci Lett* 2005;385:30–5.
22. Nakajima H, Uchida K, Kobayashi S, et al. Target muscles for retrograde gene delivery to specific spinal cord segments. *Neurosci Lett* 2008;435:1–6.
23. Xu K, Uchida K, Nakajima H, et al. Targeted retrograde transfection of adenovirus vector carrying brain-derived neurotrophic factor gene prevents loss of mouse (*twy/twy*) anterior horn neurons in vivo sustaining mechanical compression. *Spine* 2006;31:1867–74.
24. Miyake S, Makimura M, Kanegae Y, et al. Efficient generation of recombinant adenoviruses using adenovirus DNA-terminal protein complex and a cosmid bearing the full-length virus genome. *Proc Natl Acad Sci USA* 1996;93:1320–4.
25. Nakahara S, Yone K, Setoguchi T, et al. Changes in nitric oxide and expression of nitric oxide synthase in spinal cord after acute traumatic injury in rats. *J Neurotraum* 2002;19:1467–74.
26. McDonald JW, Liu XZ, Qu Y, et al. Transplanted embryonic stem cells survive, differentiate and promote recovery in injured rat spinal cord. *Nat Med* 1999;4:291–7.
27. Dergham P, Ellezam B, Essagian C, et al. Rho signaling pathway targeted to promote spinal cord repair. *J Neurosci* 2002;22:6570–7.
28. Blesch A, Lu P, Tuszynski MH. Neurotrophic factors, gene therapy, and neural stem cells for spinal cord repair. *Brain Res Bull* 2002;57:83–8.
29. Hermens WT, Verhaagen J. Viral vectors, tools for gene transfer in the nervous system. *Prog Neurobiol* 1998;55:399–432.
30. Boulis NM, Turner DE, Imperiale MJ, et al. Neuronal survival following remote adenovirus gene delivery. *J Neurosurg Spine* 2002;96:212–9.
31. Horner PJ, Power AE, Kempermann G, et al. Proliferation and differentiation of progenitor cells throughout the intact adult rat spinal cord. *J Neurosci* 2000;20:2218–28.
32. Ishii K, Toda M, Nakai Y, et al. Increase of oligodendrocyte progenitor cells after spinal cord injury. *J Neurosci Res* 2001;65:500–7.
33. Zai LJ, Wrathall JR. Cell proliferation and replacement following contusive spinal cord injury. *Glia* 2005;50:247–57.
34. Haase G, Pettmann B, Vigne E, et al. Adenovirus-mediated transfer of the neurotrophin-3 gene into skeletal muscle of pmn mice: therapeutic effects and mechanisms of action. *J Neurol Sci* 1998;160:S97–105.
35. Kishino A, Ishige Y, Tatsuno T, et al. BDNF prevents and reverses adult rat motor neuron degeneration and induces axonal outgrowth. *Exp Neurol* 1997;144:273–86.
36. Giehl KM, Rohrig S, Bonatz H, et al. Endogenous brain-derived neurotrophic factor and neurotrophin-3 antagonistically regulate survival of axotomized corticospinal neurons in vivo. *J Neurosci* 2001;21:3492–502.
37. Koda M, Murakami M, Ino H, et al. Brain-derived neurotrophic factor suppresses delayed apoptosis of oligodendrocytes after spinal cord injury in rats. *J Neurotrauma* 2002;19:777–85.
38. de Groot DM, Coenen AJ, Verhofstad A, et al. In vivo induction of glial cell proliferation and axonal outgrowth and myelination by brain-derived neurotrophic factor. *Mol Endocrinol* 2006;20:2987–98.
39. Nakajima H, Uchida K, Kobayashi S, et al. Rescue of rat anterior horn neurons after spinal cord injury by retrograde transfection of adenovirus vector carrying brain-derived neurotrophic factor gene. *J Neurotrauma* 2007;24:703–12.

40. Springer JE, Azbill RD, Knapp PE. Activation of the caspase-3 apoptotic cascade in traumatic spinal cord injury. *Nat Med* 1999;5:943–6.
41. Yoshino O, Matsuno H, Nakamura H, et al. The role of Fas-mediated apoptosis after traumatic spinal cord injury. *Spine* 2004;29:1394–404.
42. Casha S, Yu WR, Fehlings MG. Oligodendroglial apoptosis occurs along degenerating axons and is associated with Fas and p75 expression following spinal cord injury in the rat. *Neuroscience* 2001;103:203–18.
43. Dasari VR, Spomar DG, Cady C, et al. Mesenchymal stem cells from rat bone marrow downregulate caspase-3-mediated apoptotic pathway after spinal cord injury in rats. *Neurochem Res* 2007;32:2080–93.
44. Citron BA, Arnold PM, Sebastian C, et al. Rapid upregulation of caspase-3 in rat spinal cord after injury: mRNA, protein, and cellular localization correlates with apoptotic cell death. *Exp Neurol* 2000;166:213–26.
45. Knoblach SM, Huang X, VanGelderen J, et al. Selective caspase activation may contribute to neurological dysfunction after experimental spinal cord trauma. *J Neurosci Res* 2005;80:369–80.
46. Keirstead HS, Levine JM, Blakemore WF. Response of the oligodendrocyte progenitor cell population (defined by NG2 labeling) to demyelination of the adult spinal cord. *Glia* 1998;22:161–70.
47. Polite A, Reynolds R. NG2-expressing cells as oligodendrocyte progenitors expressing in the normal and demyelinated adult central nervous system. *J Anat* 2005;207:707–16.
48. Levine JM, Reynolds R. Activation and proliferation of endogenous oligodendrocyte precursor cells during ethidium bromide-induced demyelination. *Exp Neurol* 1999;160:333–47.
49. Van't Veer A, Du Y, Fischer TZ, et al. Brain-derived neurotrophic factor effects on oligodendrocyte progenitors of the basal forebrain are mediated through trkB and the MAP kinase pathway. *J Neurosci Res* 2008;87:69–78.
50. McTiger DM, Horner PJ, Strokes BT, et al. Neurotrophin-3 and brain-derived neurotrophic factor induce oligodendrocyte proliferation and myelination of regenerating axons in the contused adult rat spinal cord. *J Neurosci* 1998;18:5354–65.

JOURNAL OF NEUROTRAUMA 27:2283–2294 (December 2010)

DOI: 10.1089/neu.2009.1144

Interferon-γ Decreases Chondroitin Sulfate Proteoglycan Expression and Enhances Hindlimb Function after Spinal Cord Injury in Mice

Takayuki Fujiyoshi,[1,2] Takekazu Kubo,[1] Carmen C.M. Chan,[1] Masao Koda,[2] Akihiko Okawa,[2] Kazuhisa Takahashi,[2] and Masashi Yamazaki[2]

Abstract

Glial cells, including astrocytes and macrophages/microglia, are thought to modulate pathological states following spinal cord injury (SCI). In the present study, we evaluated the therapeutic effects of interferon-γ (IFN-γ), which is one of the cytokines regulating glial function, in a mouse contusive SCI model. We found that intraperitoneal injection of IFN-γ significantly facilitated locomotor improvement following SCI. Immunohistochemistry demonstrated that IFN-γ decreased the accumulation of chondroitin sulfate proteoglycans (CSPGs), which are critical axon outgrowth inhibitors produced by reactive astrocytes in the injured central nervous system (CNS). Quantitative real-time polymerase chain reaction (RT-PCR) and Western blotting demonstrated that neurocan, one of several CSPGs, was reduced in the spinal cords of IFN-γ-treated mice compared to vehicle-treated mice. Consistently, IFN-γ inhibited the production of neurocan from activated astrocytes *in vitro*. In addition, IFN-γ treatment enhanced the number of serotonin-positive nerve fibers and myelinated nerve fibers around the lesion epicenter. We also found that glial cell line-derived neurotrophic factor (GDNF) and insulin-like growth factor-1 (IGF-1) were upregulated post-SCI following IFN-γ treatment. Our results indicate that IFN-γ exhibits therapeutic effects in mouse contusive SCI, presumably by reducing CSPG expression from reactive astrocytes and increasing the expression of neurotrophic factors.

Key words: astrocyte; interferon-γ; chondroitin sulfate proteoglycan; macrophage; microglia; neurotrophic factors; spinal cord injury

Introduction

Injured axons in the central nervous system (CNS) regenerate poorly compared to those of the peripheral nervous system (PNS). Subsequent to spinal cord injury (SCI), the lack of axonal regeneration results in permanent functional deficits. Traumatic injury of the spinal cord causes the recruitment of glial cells including astrocytes and macrophages/microglia to the injured site, and these glial cells play positive and negative roles in axonal regeneration and functional recovery post-SCI (Donnelly and Popovich, 2008; Popovich and Longbrake, 2008; Yiu and He, 2006). Reactive astrocytes at the injured site are detrimental to axonal regeneration post-SCI, since they form a glial scar that constitutes a physical barrier to axon regeneration. They also produce chondroitin sulfate proteoglycans (CSPGs), that are potent axon outgrowth inhibitors (McKeon et al., 1991, 1999; Smith and Strunz, 2005; Yiu and He, 2006). It has been suggested that the blockade of the inhibitory effects of CSPGs is of potential therapeutic value in the treatment of SCI. Intrathecal infusion of chondroitinase ABC, which is a bacterial enzyme that cleaves glycosaminoglycan side chains on CSPGs, into the injured spinal cord has been demonstrated to overcome the inhibitory effect of CSPGs, and results in axon regrowth and functional recovery in rodents (Barritt et al., 2006; Bradbury et al., 2002).

Macrophages/microglia are also reported to play roles in the pathogenesis of CNS injuries. The beneficial effects of macrophages/microglia include the clearance of axon and myelin debris by phagocytic action/protease secretion, and the promotion of axon elongation/neuronal survival by the secretion of neurotrophic factors (Donnelly and Popovich, 2008; Jones et al., 2005; Popovich and Longbrake, 2008; Schwartz et al., 1999; Shechter et al., 2009). However, it has been suggested that the activation of macrophages/microglia after CNS injury is less efficient than that of macrophages after

Departments of [1]Neurobiology and [2]Orthopaedic Surgery, Graduate School of Medicine, Chiba University, Chiba, Japan.

PNS injury, and that this might be partly attributable to the deficiency of appropriate regeneration of the injured CNS (Schwartz et al., 1999). It is of interest that the implantation of activated macrophages promotes axonal growth and functional recovery following CNS injury (Lazarov-Spiegler et al., 1996; Rapalino et al., 1998). Conversely, the excessive inflammation associated with tissue injuries mainly induced by macrophages/microglia can also be detrimental to recovery post-SCI (Donnelly and Popovich, 2008; Jones et al., 2005; Popovich and Longbrake, 2008). Inflammatory cytokines such as tumor necrosis factor-α (TNF-α) and/or interleukin-1 (IL-1) expressed by activated macrophages/microglia induce neurodegeneration following SCI (Genovese et al., 2006; Lee et al., 2000; Nesic et al., 2001). A recent report showed that inflammation itself is required for spinal cord repair (Stirling et al., 2009). Thus anti-inflammatory cytokines do not always promote recovery after SCI, and appropriate doses of proinflammatory cytokines might be helpful for the SCI repair process.

In this study, we demonstrate that a proinflammatory cytokine, interferon-γ (IFN-γ), which modulates the activities of both astrocytes and macrophages/microglia and is clinically available for the treatment of mycosis fungoides in humans, has therapeutic effects on an experimental mouse contusion model of SCI.

Methods

The mouse animal model of spinal cord injury

Adult female C57BL/6 mice (8–10 weeks old) were anesthetized with 1–1.2% halothane in oxygen. Following dorsal laminectomy (T9–T10 level), the spinal cord was contused (60 kdyn) using an Infinite Horizon Impactor (Precision Systems & Instrumentation, West Monroe, LA), as previously described (Koda et al., 2007; Nishio et al., 2007). The muscle and skin layers were then sutured. The bladder was expressed by manual abdominal pressure every day until 2 weeks post-injury. Food and water were provided *ad libitum*. All animals were treated and cared for in accordance with the Chiba University School of Medicine guidelines pertaining to the treatment of experimental animals.

IFN-γ treatment

Immediately following SCI, the mice received an IP injection of 1.0×10^4 U recombinant mouse IFN-γ (R&D Systems, Minneapolis, MN) diluted in 500 μL phosphate-buffered saline (PBS) or 500 μL vehicle (PBS) as a control, every day for 14 days. Prior to IP injection, we expressed their bladders manually, and measured body weight and the amount of residual urine.

Behavioral analysis

Hindlimb motor function was evaluated using the Basso mouse scale (BMS) open field locomotor test, in which the scores range from 0 to 9. BMS scores were recorded at 1, 3, 5, 7, 10, 14, 21, 28, 35, and 42 days following SCI by two independent examiners. We assessed hindlimb motion, mainly in order to determine whether the mouse could coordinately move and step. If there were differences in the BMS score between the right and left hindlimbs, we took the average of the two scores.

Tissue preparation and immunohistochemistry

For immunohistochemistry, the animals were sacrificed and perfused with 4% paraformaldehyde in 0.2 M phosphate buffer (pH 7.4) at 10 days (early phase) and 6 weeks (chronic phase) post-injury, and preserved spinal cord tissues were collected. The whole spine was dissected out and post-fixed in 4% paraformaldehyde for 24 h at 4°C. Next, the spinal cord was removed from the vertebral column and retained for 48 h in 30% sucrose at 4°C for cryoprotection. The spinal cord was embedded in Tissue-Tek OCT obtained from Sakura Finetechnical Co. Ltd. (Tokyo, Japan), and immediately frozen on dry ice at −80 °C. A series of 20-μm sagittal sections as well as cross-sections were cut on a cryostat and mounted on poly-L-lysine (PLL)-coated Superfrost-Plus slides purchased from Matsunami Glass (Osaka, Japan), and desiccated overnight. After washing three times with PBS, all sections were blocked in PBS containing 5% goat serum and 0.3% Triton X-100 for 1 h at room temperature. The sections were then incubated with primary antibodies overnight at 4°C, washed three times with PBS, and incubated with fluorescein-conjugated secondary antibodies for 1 h at room temperature. The sections were then rinsed three times in PBS and mounted. For primary antibodies, we used monoclonal anti-CD11b (1:400; BD Biosciences Pharmingen, San Diego, CA), monoclonal anti-GFAP (1:500; Sigma-Aldrich, St. Louis, MO), monoclonal anti-CSPG (1:400; Sigma-Aldrich), and monoclonal anti-serotonin (1:400; Sigma-Aldrich). Luxol fast blue (LFB) staining of spinal cord cross-sections was performed in order to measure the area of spared myelinated nerve fibers in the white matter. Immunohistochemistry using each antibody was performed simultaneously to equalize the variability of staining, and all of the slides underwent LFB staining simultaneously to equalize the variability of staining.

Histological assessment

Using spinal cord sections collected 10 days post-injury, we examined the distribution of macrophages/microglia, reactive astrocytes, and the expression of CSPGs. Every fifth section of the central portion of the spinal cords was serially mounted. At least four samples, each at 80-μm intervals within 320 μm of the center of the lesion site, were mounted on a slide and evaluated by immunohistochemistry as described above.

Using spinal cord sections collected 6 weeks post-injury, we determined the number of regenerated or spared neuronal fibers by staining serotonin fibers. Descending serotonergic fibers mainly derived from the raphe-spinal tract are thought to be important for locomotor control (Deumens et al., 2005). To confirm the axonal regeneration/sparing induced by IFN-γ treatment, we performed immunohistochemistry for serotonin to count the number of serotonin-positive fibers. Every fourth section of the central portion of the spinal cords was serially mounted. At least four samples, each at an 80-μm interval within 320 μm of the center of the lesion site, were mounted on a slide and evaluated for serotonin immunohistochemistry as described above. Lines were drawn perpendicular to the long axis of the spinal cord at the epicenter, and at 1, 2, and 3 mm rostral and caudal to the epicenter. The number of serotonin-positive fibers that traversed each line was counted.

We also assessed re-myelination or spared myelin by LFB staining in transverse sections. At least four samples, each at an 80-μm interval within 320 μm, were isolated from the epicenter, as were segments 0.6 mm, 1.2 mm, and 1.8 mm rostral or caudal to the lesion epicenter.

The number of cells was determined by immunoreactivity (fluorescence intensity) using Scion Image computer analysis software (Scion Corporation, Medford, MA), and Photoshop 7.0 software (Adobe Systems, San Jose, CA).

Real-time quantitative polymerase chain reaction

Total RNA from the injured spinal cords (6-mm segments including the lesion epicenter; the samples were near the region assessed by immunohistochemistry) was isolated 1 week after SCI using an RNeasy Kit (Qiagen, Hilden, Germany), and cDNA was obtained using reverse transcriptase (GE Healthcare, Buckinghamshire, U.K.). For the quantitative analysis of mRNA expression of neurotrophic factors, proinflammatory cytokines, and neurocan, the cDNA was used as the template in a TaqMan real-time PCR assay (ABI Prism 7500 Sequence Detection System; Applied Biosystems, Foster City, CA), according to the manufacturer's protocol. Specific primers and probes for the TaqMan real-time PCR assay were purchased from Applied Biosystems. The following TaqMan probes were used in this study: MCP-1 (Applied Biosystems catalog no. Mm99999056_m1), CCR-2 (no. Mm99999051_gH), neurocan (no. Mm00484007_m1), GDNF (no. Mm00599849_m1), IGF-1 (no. Mm00439561_m1), BDNF (no. Mm00432069_m1), and NT-3 (no. Mm00435413_s1).

Enzyme-linked immunosorbent assay (ELISA)

Injured spinal cords (6-mm segments including the lesion epicenter; the sample was near the same region assessed by immunohistochemistry) were homogenized in homogenization buffer (50 mM Tris-HCl [pH 7.4], 150 mM NaCl, and 1% Triton X-100) containing a protease inhibitor cocktail (complete; Roche Diagnostics, Basel, Switzerland). Homogenates were cleared by centrifugation at 14,000 rpm for 10 min at 4°C. Protein concentration of the supernatants was measured with Bio-Rad Dc Protein Assay Reagents (Bio-Rad Laboratories, Hercules, CA), and the protein concentration was adjusted to 1 mg/mL by diluting the supernatants with a homogenization buffer. IFN-γ in the supernatants was quantified with an immunoassay kit from Bender MedSystems (Vienna, Austria), following the manufacturer's protocol. In order to determine if IP-administrated IFN-γ reached the injured spinal cord, we examined IFN-γ concentration with ELISA at 5, 10, and 14 days post-SCI.

Western blotting

Homogenates of injured spinal cords were prepared as described above in the ELISA section. After centrifugation, protein concentration of the supernatants was adjusted to 1 mg/mL. For the detection of neurocan, the supernatants were digested by chondroitinase ABC (Seikagaku Corp., Tokyo, Japan) for 3 h at 4°C, and mixed with an equal volume of a 2×sample buffer (250 mM Tris-HCl, 4% sodium dodecyl sulfate [SDS], 20% glycerol, 0.02% bromophenol blue, and 10% β-mercaptoethanol). For the detection of GFAP, Nogo A, and semaphorin 3A, the supernatants were mixed with an equal volume of a 2×sample buffer. After boiling for 5 min, equal volumes of the samples were subjected to 5% (neurocan) or 10% (GFAP, Nogo A, and semaphorin 3A) SDS-polyacrylamide gel electrophoresis (SDS-PAGE) under reducing conditions, and the proteins were transferred to a polyvinylidene difluoride membrane (Immobilon-P; Millipore Corp., Billerica, MA). After blocking of the membrane with PBS containing 5% skim milk and 0.05% Tween 20, the membrane was reacted with anti-neurocan (Seikagaku Corp.), anti-GFAP (Sigma-Aldrich), anti-Nogo A (Santa Cruz Biotechnology, Santa Cruz, CA), or anti-semaphorin 3A (Santa Cruz Biotechnology) antibodies. For detection, a horseradish peroxidase-conjugated secondary antibody (Cell Signaling Technology, Beverly, MA), and an ECL chemiluminescence system (GE Healthcare) were used. Quantification of protein bands was performed using Scion image software.

Astrocyte culture

Primary astrocyte cultures were prepared from newborn mice at post-natal day 1 (P1). The upper portion of the skull was opened and the meninges were carefully removed in order to minimize contamination of the cell culture with fibroblasts. The cerebral cortices were cut into small pieces and enzymatically dissociated using 0.025% trypsin in PBS for 10 min at 37°C. Following the addition of 10% FBS and 0.5 mg/mL DNase I, the dissociated cortices were triturated and then gravity filtered through a 70-μm cell strainer. The cells were resuspended in Dulbecco's modified Eagle's medium (DMEM) plus GlutaMAX (Invitrogen Corp., Carlsbad, CA) containing 10% fetal bovine serum (FBS) and 1% penicillin/streptomycin, and then seeded onto PLL-coated 75-cm^2 tissue culture flasks. The medium was changed every 3 days until the cells were confluent. Thereafter, the flasks were shaken at 200 rpm for 6 h in order to remove the contaminating non-astrocytic cells. The astrocytes were gently trypsinized, rinsed in fresh medium containing 10% FBS, and then plated on PLL-coated four-chamber glass slides. The astrocytes were treated with 10 ng/mL transforming growth factor-β (TGF-β), purchased from PeproTech, Inc. (Rocky Hill, NJ), or 10 ng/mL epidermal growth factor (EGF; PeproTech, Inc.), in the absence or presence of 2.0×10^3 U/mL IFN-γ (R&D Systems) for 24 h, before collection of total RNA using an RNeasy Kit (Qiagen).

Statistical analysis

For all experiments with the exception of the behavioral analyses, statistical analysis was performed using the Student's *t*-test. For the behavioral analyses, BMS scores were analyzed using repeated-measures analysis of variance (ANOVA), followed by Fisher's protected least significant difference (PLSD) *post-hoc* test. For fractional BMS scores at each time point, one-way ANOVA followed by the Bonferroni/Dunn test were used. Statistical significance was set at $p < 0.05$ for fractional BMS scores. All values are the means ± standard error.

Results

Intraperitoneally-administered IFN-γ reaches the injured spinal cord

We performed ELISA for IFN-γ to determine whether intraperitoneally-administered IFN-γ can reach the injured

spinal cord. IFN-γ was almost undetectable in uninjured and injured spinal cords without IFN-γ treatment. In contrast, IFN-γ was clearly detected in the injured spinal cords with IFN-γ treatment at 5 and 10 days post-SCI, suggesting that the intraperitoneally-administered IFN-γ had reached the injured spinal cords at least until 10 days post-SCI (Fig. 1).

IFN-γ improves locomotor performance post-SCI

In order to assess the therapeutic effects of IFN-γ on a mouse contusion SCI model, IP administration of IFN-γ once a day for 14 days post-SCI was performed. We evaluated the locomotor function of hindlimbs by recording BMS scores for up to 6 weeks post-SCI. The overall BMS scores for IFN-γ-treated mice were significantly higher than those of the vehicle-treated mice, as calculated by repeated-measures ANOVA ($p < 0.01$); furthermore, at specific time points (10, 14, and 21 days) post-SCI, there were significant differences between the two groups ($p < 0.05$; Fig. 2). After 6 weeks, the vehicle-treated group's score leveled off at 2.8 ± 0.6 points, while the IFN-γ-treated group was at 4.4 ± 0.6 points, and its score appeared to continue to increase. Whereas the hindlimbs of the vehicle-treated mice exhibited only extensive ankle movement, IFN-γ-treated mice exhibited occasional plantar stepping or consistent dorsal stepping within 10 days post-SCI, suggesting that IFN-γ has therapeutic effects, even in the early phase post-injury. We also examined body weight and residual urine; however, there were no significant differences between the two groups (data not shown).

IFN-γ treatment increased the range of macrophage/microglia accumulation post-SCI

The distribution of macrophages/microglia in spinal cords following injury was examined immunohistochemically at 10 days post-SCI. At this time point, numerous CD11b-positive macrophages/microglia were seen densely clustered in the epicenter of the injured area in vehicle-treated mice, as previously reported (Kigerl et al., 2006; Sroga et al., 2003; Fig. 3A). However, the injured spinal cords of IFN-γ-treated mice exhibited a different distribution of these cells. In these mice, the accumulation of macrophages/microglia was less dense at the epicenter; instead, these cells were more widely distributed from the rostral to the caudal side of the epicenter (Fig. 3B). The mean range of the horizontal distribution of the infiltrated macrophages/microglia was 1.18 ± 0.03 mm in the vehicle-treated group, and 6.15 ± 0.96 mm in the IFN-γ-treated group (Fig. 3D), and the difference between the two groups was statistically significant ($p < 0.05$). There was a tendency for more macrophages/microglia to accumulate in the IFN-γ-treated group; however, the difference between the two groups was not statistically significant ($p = 0.08$; Fig. 3C). We attempted to determine the difference in macrophage/microglia distribution by examining the expression of chemokines that are known to affect macrophage migration. We examined the mRNA levels of MCP-1 and its receptor CCR-2 in the spinal cord at 1 week post-SCI by real-time PCR (Fig. 3E and F). The relative levels of MCP-1 and CCR-2 mRNAs were 1.9 and 3.8 times higher, respectively, in the IFN-γ-treated group than in the vehicle-treated group. To address the effects of IFN-γ treatment on the levels of proinflammatory cytokines, we checked mRNA levels of TNF-α, IL-1β, and IL-6 in the spinal cord at 1 week post-SCI by real-time PCR (Supplementary Fig. 1; see online supplementary material at http://www.liebertonline.com). There was no statistically significant difference in the levels of TNF-α, IL-1β, and IL-6 mRNA with vehicle or IFN-γ treatment, although there was a tendency toward an increase in IL-1β and IL-6 levels with IFN-γ treatment.

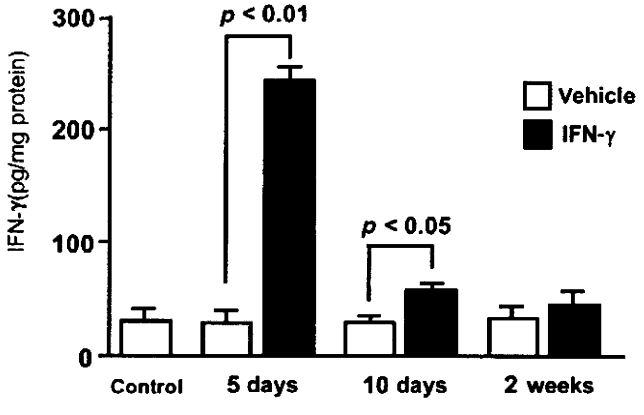

FIG. 1. Intraperitoneally-administered interferon-γ (IFN-γ) reached the injured spinal cord. We performed enzyme-linked immunosorbent assay (ELISA) for IFN-γ to determine whether intraperitoneally-administered IFN-γ could reach the injured spinal cord. IFN-γ was nearly undetectable in uninjured and injured spinal cords without IFN-γ treatment. In contrast, IFN-γ was clearly detected in the injured spinal cords with IFN-γ treatment at 5 and 10 days post-SCI, suggesting that the intraperitoneally-administered IFN-γ reached the injured spinal cords at least until 10 days post-SCI (SCI, spinal cord injury).

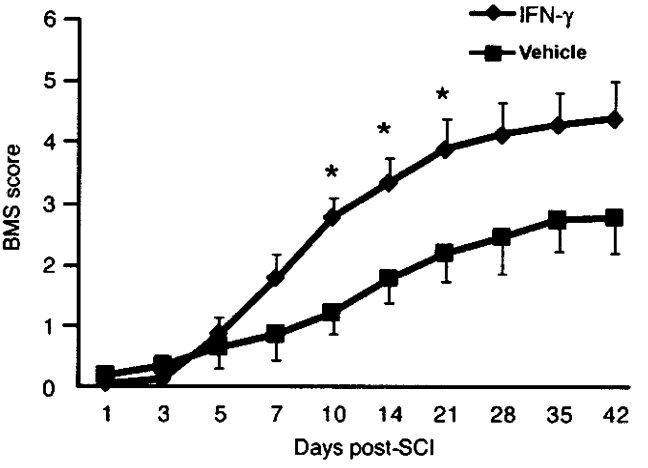

FIG. 2. Interferon-γ (IFN-γ) promotes functional recovery following spinal cord injury (SCI). Hindlimb function of mice following SCI was evaluated using the Basso mouse locomotor scale (BMS). Repetitive administration of IFN-γ for 14 days post-injury significantly enhanced hindlimb functional recovery, as assessed by repeated-measures analysis of variance (ANOVA; $p < 0.01$). After 10, 14, and 21 days post-SCI, IFN-γ-treated mice ($n = 15$) exhibited significantly better hindlimb function than vehicle-treated mice ($n = 13$; $^*p < 0.05$).